Sedimentary provenance from the evolving forearc-to-foreland Central Sakarya Basin, western Anatolia reveals multi-phase intercontinental collision

Megan A. Mueller[1], Alexis Licht[1,2], Clay Campbell[3], Faruk Ocakoğlu[4], Gui G. Akşit[1,5], Grégoire Métais[6], Pauline M. C. Coster[7], K. Christopher Beard[8,9], Michael H. Taylor[3]

[1]Department of Earth and Space Sciences, University of Washington, Seattle, Washington 98195, USA

[2]Aix-Marseille Université, CNRS, Centre de Recherche et d'Enseignement de Géosciences de l'Environnement (CEREGE), Aix-en-Provence, France

[3]Department of Geology, University of Kansas, Lawrence, Kansas 66045, USA

[4]Department of Geological Engineering, Eskişehir Osmangazi University, 26040 Eskişehir, Turkey

[5]Department of Earth Sciences, University of Oregon, Eugene, Oregon 97403, USA

[6]Centre de Recherches sur la Paléobiodiversité et les Paléoenvironnements, Muséum National d'Histoire Naturelle, 75005 Paris, France

[7]Réserve naturelle nationale géologique du Luberon, Apt, France

[8]Biodiversity Institute, University of Kansas, Lawrence, Kansas 66045, USA

[9]Department of Ecology and Evolutionary Biology, University of Kansas, Lawrence, Kansas 66045, USA

Corresponding author: Megan Mueller (megan.mueller@uconn.edu)

This manuscript is a non-peer reviewed preprint submitted to ESSOAr

Manuscript under consideration at Geochemistry, Geophysics, Geosystems

Original submission date: 10 February 2021

Key Points:

- Multi-phase intercontinental collision is identified in the western Pontides of Anatolia by changes in sediment provenance
- Sedimentary provenance indicates collision at 76 Ma and arc shut off at 70 Ma, but significant deformation was delayed until 54 Ma
- The protracted, 20 Myr duration of initial intercontinental collision can be explained three mechanisms involving changes in plate coupling

Abstract

Collision between the Pontides and Anatolide-Tauride Block along the İzmir-Ankara-Erzincan suture in Anatolia has been variously estimated from the Late Cretaceous to Eocene. It remains unclear whether this age range results from a protracted, multi-phase collision or differences between proxies of collision age and along strike. Here, we leverage the Cretaceous-Eocene evolution of the forearc-to-foreland Central Sakarya Basin system in western Anatolia to determine when and how collision progressed. New detrital zircon and sandstone petrography results indicate that the volcanic arc was the main source of sediment to the forearc basin in the Late Cretaceous. The first appearance of Pontide basement-aged detrital zircons, in concert with exhumation of the accretionary prism and a decrease in regional convergence rates indicates intercontinental collision initiated no later than 76 Ma. However, this first contractional phase does not produce thick-skinned deformation and basin partitioning until ca. 54 Ma, coeval to regional syn-collisional magmatism. We propose three non-exclusive and widely applicable mechanisms to reconcile the observed ~20 Myr delay between initial intercontinental collision and thick-skinned upper plate deformation: relict basin closure north and south of the İAES, gradual underthrusting of thicker lithosphere, and Paleocene slab breakoff. These mechanisms highlight the links between upper plate deformation and plate coupling during continental collision.

Plain Language Summary

Key to understanding the interconnectedness of Earth's systems is unraveling feedbacks between climate, biology, and tectonic plate movements. This can only be resolved within a robust timeframe of tectonic events, such as oceanic basins closure and collision of two continents. Yet, the timing of collisions is difficult to determine. We present results from western Turkey where the history of oceanic basin closure and collision from 110 to 40 million years ago (Ma) is

preserved in the sedimentary rock record. We identify three phases of oceanic closure (subduction) and continental collision. Subduction was active from at least 110 Ma through 76 Ma when sediment was derived from active volcanoes. At 76 Ma, continental deformation uplifted and eroded older rocks; this is the initial contact between colliding continents. At 54 Ma, continental deformation separated the zone of sediment deposition into two basins, the final collision phase. The 20-million-year collision duration can be explained by three changes to tectonic plate coupling. Together, we conclude that collision age discrepancies are representative of collision mechanics not a function of ill-fit comparisons. This long history of collision illuminates how the movement and amalgamation of small continents aided the migration and evolution of species.

Keywords: Anatolia, Neotethys, Intercontinental Collision, Detrital Zircon Geochronology

1. Introduction

Continental collisions across the Tethyan realm are striking by their protracted and polygenetic history, often resulting in significant discrepancies among proxies of collision age: ~40 Myr for India-Asia (65-25 Ma; Ding et al., 2005; Hu et al., 2016; Kapp & DeCelles, 2019; Najman et al., 2010) and ~20 Myr for Arabia-Eurasia (Ballato et al., 2011; Cowgill et al., 2016; Darin et al., 2018; McQuarrie et al., 2003; Okay et al., 2010). Their unusual duration and complexity have even put into question the nature of the forces driving intercontinental convergence (Alvarez, 2010; Becker & Faccenna, 2011), leading to multi-phase scenarios either involving either varying plate coupling at the subduction interface (Ballato et al., 2011; Beaumont et al., 1996; Tye et al., 2020) or the role of forearc, backarc, and other remnant basins as early buffers of deformation (Cowgill et al., 2016).

Collision age discrepancies are also found in western and central Anatolia where continental collision between the Pontides and the Anatolide-affinity Tavşanlı Zone (TVZ) and Kırşehir Block along the İzmir-Ankara-Erzincan suture (İAES) closed the Neotethys Ocean (**Figure 1**; Şengör & Yilmaz, 1981). Collision estimates along the İAES span 20 Myr from the Late Cretaceous to early Eocene based on ophiolite obduction and Barrovian metamorphism (Göncüoğlu et al., 2000; Seaton et al., 2009; Whitney et al., 2011), structural deformation (Lefebvre et al., 2013; Meijers et al., 2010; Şahin et al., 2019), magmatism (Dilek & Altunkaynak, 2009; Ersoy, Akal, et al., 2017; Kasapoğlu et al., 2016), and sedimentary basin analysis (Kaymakci

et al., 2009; Ocakoğlu et al., 2018; Okay, 2011). However, a model that encompasses the insights from all proxies is still missing.

To address this, we leverage the power of a ~50 Myr continuous depositional record from the Central Sakarya Basin system, a forearc-to-foreland basin directly north of the İAES. Integrating new sedimentary provenance data with previously published stratigraphic and provenance data reveals a multi-phase collisional evolution. The TVZ was subducted to ca. 80 km depth sometime between 95 and 85 Ma (e.g., Plunder et al., 2015; Pourteau et al., 2019) in an intra-oceanic subduction zone (Göncüoğlu et al., 2000, 2010; Sarıfakıoğlu et al., 2009, 2017) during which the Central Sakarya Basin was a forearc basin. The underthrusting of TVZ continental lithosphere beneath the Pontides initiated at 76 Ma, resulting in uplift of the accretionary complex and sediment recycling in the forearc, followed ~20 Myr later with thick-skinned deformation and basin partitioning at 54 Ma. We evaluate the timing of this protracted deformation in light of previously proposed multi-phase collision models for the Tethyan realm, including passive margin subduction, (relict) basin closure, and slab breakoff.

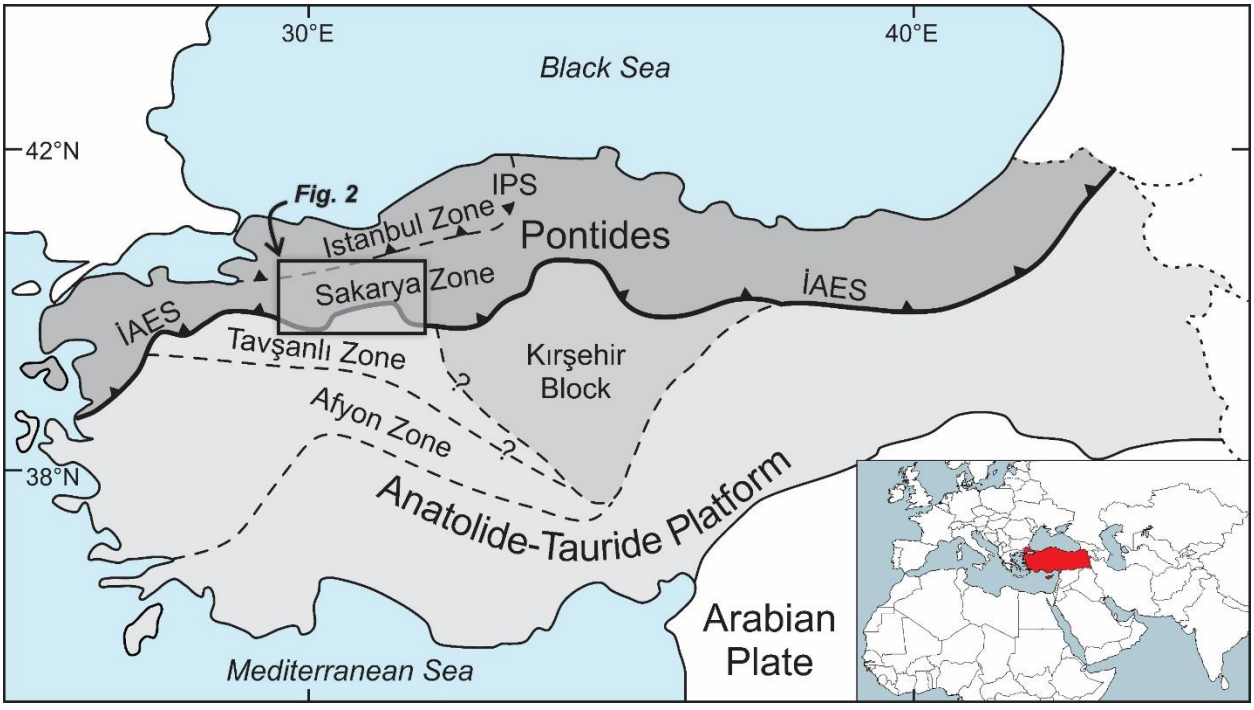

Figure 1. Simplified terrane map of Anatolia including hypothesized suture zones (dashed lines) modified from Licht et al. (2017). İAES: İzmir-Ankara-Erzincan suture zone; IPS: Intra-Pontide suture zone.

2. Background

The tectonic units in northwest Anatolia include, from north to south, the İstanbul Zone and Sakarya Zone (SKZ) of the pre-Carboniferous Eurasian-affinity Pontides, the İzmir-Ankara-Erzincan suture zone (İAES), and the Tavşanlı Zone (TVZ) of the Gondwanan-affinity Anatolides (**Figure 1**; Şengör & Yilmaz, 1981). The Pontides rifted from the Eurasian margin between 94 and 75 Ma by backarc spreading of the Black Sea (Akdoğan et al., 2017, 2019; Okay et al., 2013; Okay & Nikishin, 2015), and formed an isolated microcontinent where faunal endemism prevailed until the late Paleogene (Métais et al., 2018). The SKZ, bound to the north by the Intra-Pontide suture zone, presently occupied by the North Anatolian Fault, comprises Sakarya Zone basement units and the forearc-to-foreland Central Sakarya Basin system (**Figure 2**). The Sakarya Zone continental basement is subdivided into two units: (1) the Central Sakarya Basement (also called Söğüt metamorphics) comprising Paleozoic paragneiss, schist and amphibolite rocks intruded by Carboniferous granitoids called the Söğüt magmatics, Central Sakarya granite, or Sarıcakaya granitoid (Göncüoğlu et al., 2000; P. Ustaömer et al., 2012), and (2) the Permian-Triassic Karakaya Complex, partly metamorphosed clastic and volcanic rocks from either a rift or subduction-accretion complex setting (see Okay & Göncüoglu, 2004). The basement is intruded by the Pontide volcanic arc: Late Cretaceous plutons are found along the southern Black Sea coast from Bulgaria to Georgia (**Figure 3**) associated with northward subduction along the Pontide margin (e.g., Şengör & Yilmaz, 1981). Local Late Cretaceous volcanic centers and volcanoclastic rocks are identified within the Sakarya Zone (e.g., Duru & Aksay, 2002; Gedik & Aksay, 2002; Ocakoğlu et al., 2018; Speciale et al., 2012). The SKZ, İstanbul Zone, and TVZ are intruded by Eocene (58-41 Ma) syn-collisional plutons disputedly attributed to TVZ slab breakoff, lithospheric delamination, or anatexis of the lower crust (Harris et al., 1994; van Hinsbergen et al., 2010; Kasapoğlu et al., 2016; Mueller et al., 2019; P. Ustaömer et al., 2009). The Central Sakarya Basin system is divided into the Jurassic-Eocene forearc-to-foreland Central Sakarya Basin (CSB; also called the Mudurnu-Göynük Basin) to the north and the Eocene broken foreland Sarıcakaya Basin (SB) to the south (e.g., Mueller et al., 2019; Ocakoğlu et al., 2007; Okay et al., 2001). The basement-involved Tuzaklı-Gümele Thrust (also termed the Söğüt Thrust and Nallıhan Thrust; **Figure 2**) structurally partitioned the CSB by the early Eocene and flexural loading formed the SB. Sakarya Zone basement units are exposed in the hanging wall (Duru & Aksay, 2002; Gedik & Aksay, 2002). The SB contains Eocene terrestrial deposits and hosts one of the Eocene volcanic

belts (Kasapoğlu et al., 2016; Yildiz et al., 2015). The fold-thrust belt is located within the basin system; W-E and SW-NE striking oblique thrust faults and folds deform Jurassic through Eocene units. Thin-skinned thrust faults in the CSB are likely reversed extensional faults from a phase of Santonian-Campanian extension (**Figure 2**; Ocakoğlu et al., 2018).

The SKZ is bound to the south by the İAES, a highly deformed accretionary complex containing obducted ophiolite, ophiolitic mélange and metamorphic rocks (e.g., Göncüoğlu et al., 2000, 2010). To the south, the TVZ is generally considered the passive margin of the northernmost Gondwana-derived Anatolide-Tauride Block (e.g., Okay, 2011; Okay et al., 1996). Platform carbonates and passive margin clastics were subducted and metamorphosed to blueschist facies between 92 and 83 Ma (e.g., Okay et al., 1998; Plunder et al., 2015; Sherlock et al., 1999; Whitney et al., 2011), exhumed sometime 85-60 Ma (Seaton et al., 2009; Sherlock et al., 1999; Whitney & Davis, 2006), then underwent Barrovian-type metamorphism from 63 to 57 Ma (Seaton et al., 2009; Whitney et al., 2011). The blueschist unit is tectonically overlain by metamorphosed accretionary complexes (Plunder et al., 2013) and obducted ophiolites and mélange (Göncüoğlu, 2010; Yaliniz et al., 2000). The western Anatolian ophiolites have metamorphic sole ages between 101 and 88 Ma (Dilek et al., 1999; Harris et al., 1994; Pourteau et al., 2019) and are cut by 92 to 90 Ma mafic dikes (Dilek et al., 1999), and, therefore, were obducted sometime after ~90 Ma during pre-collisional TVZ subduction (Okay & Whitney, 2010; Robertson et al., 2009). The blueschists and ophiolites are intruded by Eocene granodiorites (Harris et al., 1994) and unconformably overlain by lower Eocene shallow marine limestones and siliciclastic rocks (Baş, 1986; Özgen-Erdem et al., 2007) and lower-to-middle(?) Eocene continental deposits (Turhan, 2002). Herein we refer to TVZ subduction as the phase when TVZ continental lithosphere was subducted beneath overlying oceanic lithosphere, whereas underthrusting refers to the phase when TVZ continental lithosphere was thrust beneath the upper plate Pontide continental lithosphere.

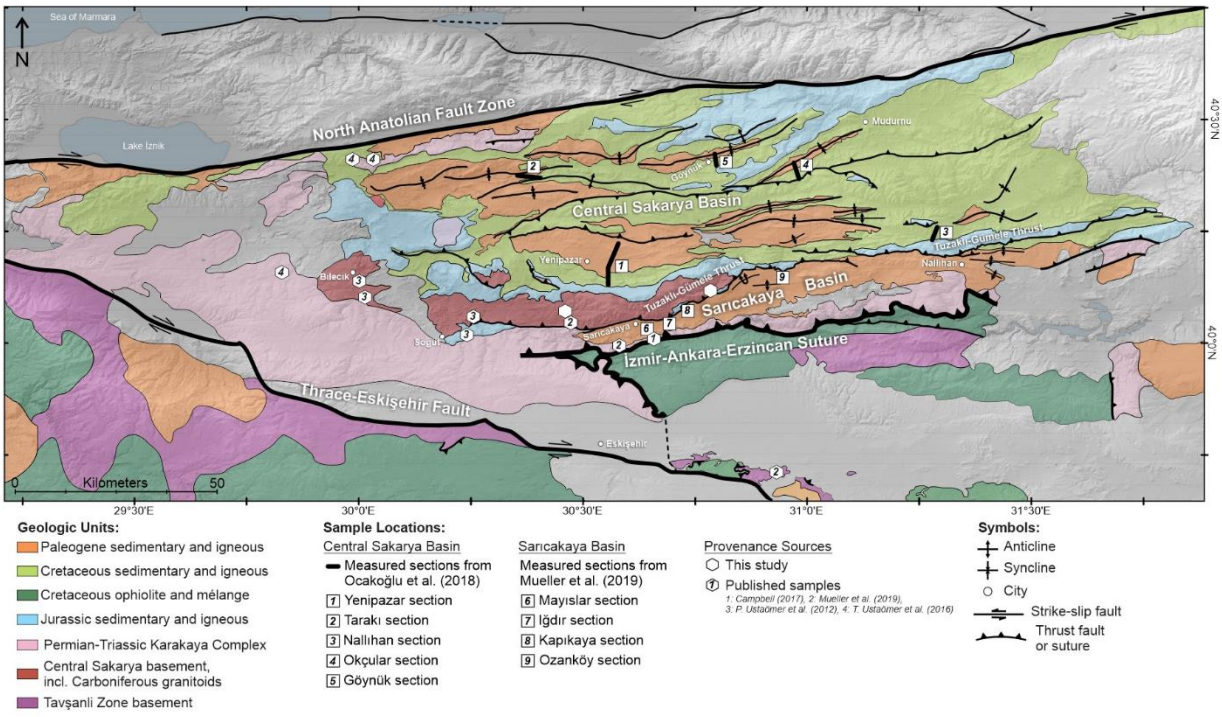

Figure 2. Simplified geologic map of northwestern Anatolia (after Aksay et al., 2002; Duru & Aksay, 2002; Gedik & Aksay, 2002; Şahin et al., 2019; Timur & Aksay, 2002; Turhan, 2002). See Figure 1 for location. Note that some published Karakaya Complex samples are west of the displayed map area.

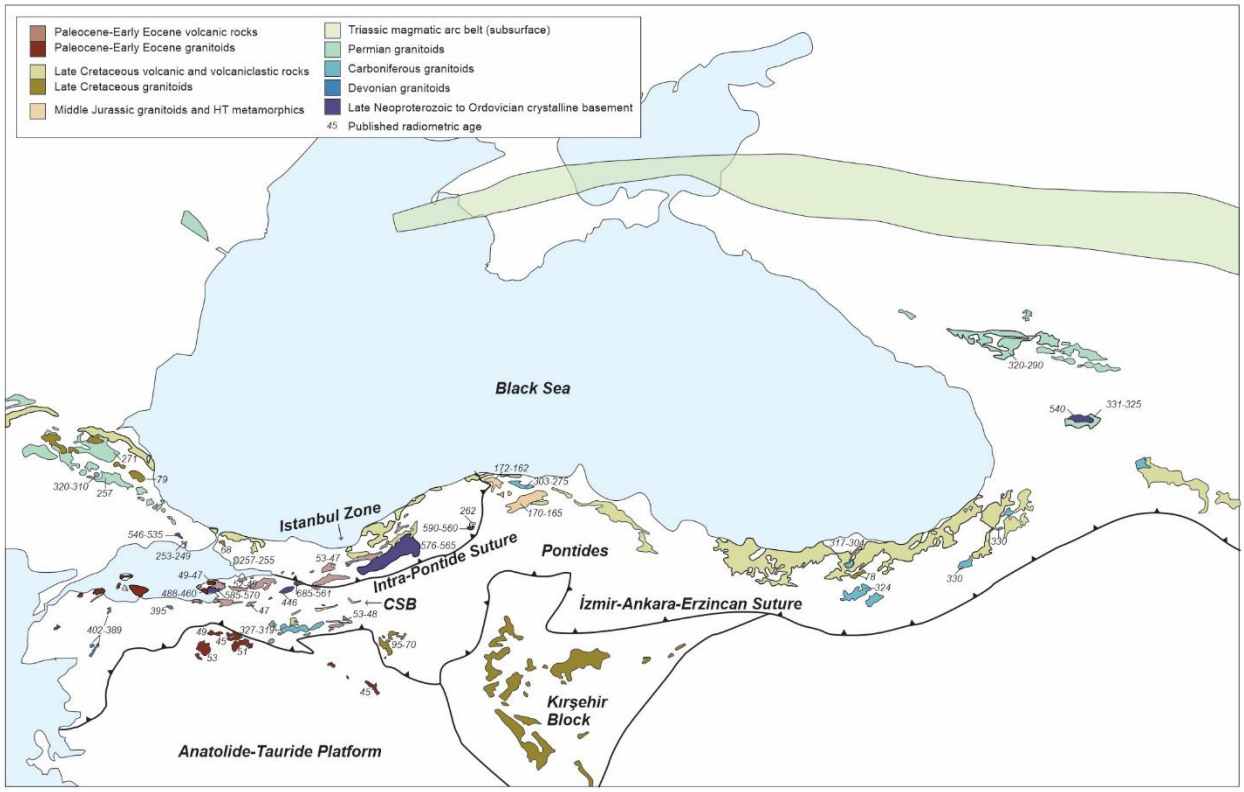

Figure 3. Outcrops and isotopic ages of late Neoproterozoic through Eocene magmatic and metamorphic rocks adapted from Akdoğan et al. (2017), Ersoy, Akal, et al. (2017), and Okay & Nikishin (2015) and references therein. The Late Cretaceous volcanoclastics in the southern CSB are included (see Ocakoğlu et al., 2018; Duru & Aksay, 2002; Gedik & Aksay, 2002).

3. Central Sakarya Basin Stratigraphy

Jurassic through Eocene sedimentation is preserved in the Central Sakarya Basin (e.g., Aksay et al., 2002). **Figure 4** displays stratigraphic columns with biostratigraphic ages for the Upper Cretaceous through Eocene units along two transects across the CSB (after Ocakoğlu et al., 2018).

Unconformably overlying Sakarya Zone basement units are the Jurassic through Lower Cretaceous series of shallow water platform carbonates (Bilecik Fm.), pelagic micrites and calciturbidites (Soğukçam Fm.), and interbedded volcanics (Mudurnu Fm.) (Altiner et al., 1991; Genç & Tüysüz, 2010). The CSB formed as a rift basin, as indicated by overall basin deepening

facies and bimodal Jurassic volcanism (Altiner et al., 1991; Genç & Tüysüz, 2010; Göncüoğlu et al., 2000), bounded by two branches of the Neotethys Ocean: the Intra-Pontide Ocean to the north and the İzmir-Ankara Ocean to the south. There is uninterrupted Jurassic through Paleocene sedimentation in the eastern CSB (e.g., Nallıhan transect in **Figure 4**), whereas much of the Albian through Lower Campanian section is missing in the western CSB (e.g., Okay et al., 2001). The Albian-Lower Campanian sequence exhibits complex basin architecture, for which Ocakoğlu et al. (2018) provided updated biostratigraphic ages and tectonostratigraphic interpretations. This interval includes siliciclastic turbidites and pelagic mudstones (Yenipazar and Seben Formations) interfingered with the Albian-Turonian Üzümlü Member volcaniclastics and submarine lava flows, the Santonian-Lower Campanian Değirmenözü Formation pelagic carbonates, and lower to middle Campanian Eymür Member submarine fan deposits. The shallow marine to deltaic Paleocene Taraklı Formation conformably overlies the Yenipazar Formation. The shelf was likely located near the Nallıhan section, where deltaic progradation began sometime early Paleocene, then deltaic sands and muds reached the northern Taraklı section in the late Paleocene when sedimentation rates were briefly extremely rapid (Ocakoğlu et al., 2018).

In the Yenipazar section in the west, the Kızılçay Fm. unconformably overlies the Yenipazar Fm, whereas in the Nallıhan section in the east, the Kızılçay Fm. conformably overlies the Taraklı Fm. The shoaling sequence is overlain by coal beds, cross bedded sandstones and caliches of the Kızılçay Fm. (Ocakoğlu et al., 2018). Ostracod fauna indicate a Ypresian age (Ocakoğlu et al., 2018). In the proximal Nallıhan and Yenipazar sections, fluvial conglomerates contain reworked Upper Cretaceous clasts and marine microfauna, and cross beds and clast imbrications indicate paleocurrent directions to the NW and NE. The Kızılçay Fm. grades northward into the Yenipazar Fm. where prograding delta-front sandstones are present in the Akdoğan section (Ocakoğlu et al., 2018). The Kızılçay Fm. is likely correlative with the Ypresian to Lutetian(?) continental clastics and volcanics of the Mihalgazi Fm. in the Sarıcakaya Basin (Gedik & Aksay, 2002; Kasapoğlu et al., 2016; Mueller et al., 2019; Şahin et al., 2019; Yildiz et al., 2015). The coarse marine clastics, alternating sands and muds, and turbidite deposits of the Kabalar Mbr. of the Kızılçay Fm. and the conformably overlying Güvenç Fm., Çataltepe Fm., and Halidiye Fm. record a Ypresian through early Bartonian marine transgression (Ocakoğlu et al., 2012, 2018). The late Lutetian maximum flooding surface is recorded in sedimentary basins across the Black Sea region, including Anatolia, Crimea and the Caucasus (e.g., Licht et al., 2017; Lygina

et al., 2016; MTA, 2002; E. Özcan et al., 2019; Racey, 2001). The Gemiciköy Fm. comprises mudstone and cross-bedded sandstones that coarsen upward to fluvial conglomerates with clasts of reworked Cretaceous-Paleocene units (Ocakoğlu et al., 2007); it only crops out north of Yenipazar where it conformably overlies the Güvenç Fm. (Gedik & Aksay, 2002; Ocakoğlu et al., 2018).

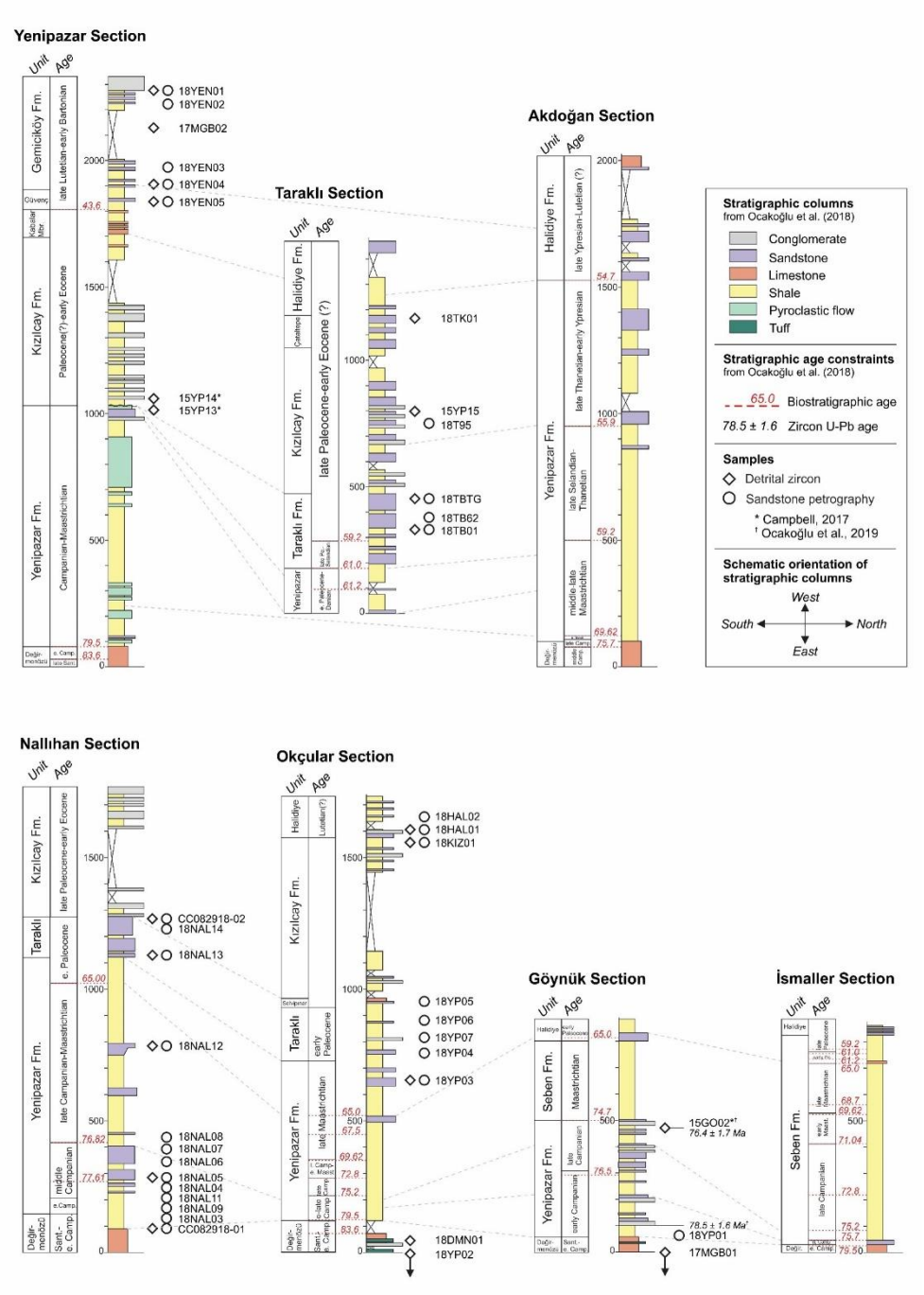

Figure 4. Simplified Upper Cretaceous through Eocene lithostratigraphic diagram of the Central Sakarya Basin, including sample locations. The stratigraphic columns and biostratigraphic ages are from Ocakoğlu et al. (2018). See Figure 2 for stratigraphic column locations.

4. Methods

We collected 37 new sandstone samples from Cretaceous through Eocene strata in the CSB and 2 new gneiss samples from the Central Sakarya Basement (**Figure 4**,

see **ESSOAr supplemental files:**

Table 1). The sandstone samples were collected along five published measured sections from two proximal (south) to distal (north) transects through the CSB (**Figure 2**; Ocakoğlu et al., 2018). The provenance of sandstone samples was evaluated using detrital zircon (DZ) U-Pb geochronology and sandstone petrography.

For the new CSB samples, heavy mineral separation, analysis, and data reduction followed the University of Washington TraceLab protocol (Licht et al., 2018; Shekut & Licht, 2020). Zircons were separated following standard heavy mineral separation procedures. A minimum of 140 grains per sample were randomly selected, mounted with reference materials, imaged in a backscattered electron detector with a scanning electron microscope, and analyzed using a quadrupole laser ablation-inductively coupled plasma-mass spectrometer (LA-ICP-MS). The data were reduced in *Iolite* using the Geochron Data Reduction Scheme (Paton et al., 2011). Individual zircons with abnormal patterns in raw signal intensity, >20% discordance, or >5% reverse discordance are reported in the supporting information but are excluded from analyses and interpretations (following Gehrels, 2012, 2014). All zircon U-Pb ages are presented uncorrected for common lead (Shekut & Licht, 2020), and the data are presented as probability density functions and kernel density estimates with an optimized fixed bandwidth, all plotted using *detritalPy* (Sharman et al., 2018).

The ages of the sedimentary samples were constrained by published biostratigraphic and volcanic zircon U-Pb ages along the measured sections (Campbell, 2017; Ocakoğlu et al., 2018). Maximum depositional ages, calculated using the youngest cluster of 2 or more ages with overlapping 2s uncertainties (Sharman et al., 2018), are included in Dataset S1 but do not provide any new constraint on sample ages.

We characterize the zircon age signature of potential sediment sources from new Central Sakarya Basement bedrock samples alongside published Central Sakarya Basement, Karakaya Complex, and İAES bedrock and modern river samples (Campbell, 2017; Mueller et al., 2019; P.

Ustaömer et al., 2012; T. Ustaömer et al., 2016). We also include crystallization ages of Cretaceous-Eocene plutons in Central and Western Anatolia compiled in Schleiffarth et al. (2018). The two new basement samples and one CSB sample (15YP15) were analyzed at the University of Kansas Isotope Geochemistry Laboratory following the analytical protocol outlined in Campbell (2017). Zircons were separated following standard methods, mounted with international standards, and analyzed in a high resolution sector-field LA-ICP-MS. Data were reduced in *Iolite* (Paton et al., 2011) and *ET_Redux* (McLean et al., 2016) and are presented uncorrected for common lead.

We further characterize sedimentary provenance using petrographic analysis of sandstone samples (N=31). Thin sections were made by National Petrographic Service, Inc. and at least 400 framework grains per sample were point counted according to the Gazzi-Dickinson method (Dickinson, 1985). The new CSB sandstone modal composition data are presented as ternary diagrams (Triplot; Graham & Midgley, 2000) and interpreted following standard source fields (Dickinson, 1985; Dickinson & Suczek, 1979).

5. Provenance Results and Interpretation

5.1. Provenance Results

New DZ data (N=19; n=3188) are presented with published DZ data (N=13, n=1457; **Table 1**). Detrital zircon distributions of potential sources and basin samples are given in **Figure 5** and **Figure 6**, respectively. To facilitate comparison, distributions are colored according to the ages of known late Neoproterozoic through Eocene volcanic and plutonic outcrops across the Black Sea region (**Figure 3**). Sandstone petrography results of new CSB samples are displayed in **Figure 7**.

New (N=2, n=169) and published (n=1763) bedrock, detrital, and modern river zircon U-Pb ages characterize the zircon signature of basement units and volcanic arcs (**Figure 5; Table 1**). The Central and Eastern Anatolian volcanic arc is characterized by 30-56 Ma and 67-99 Ma age peaks. The Karakaya Complex samples are characterized by 200-250 and 325 Ma populations, and, additionally, the modern river sample (17RIVER01) draining the İAES contains minor Eocene, Late Cretaceous, Triassic, and Paleozoic populations. The Central Sakarya Basement bedrock samples exhibit a prominent ~325 Ma peak, and the oldest samples include 375-500 Ma age populations; the metasedimentary sample (‘SgtMeta’ from Ustaömer et al., 2012) contains a

range of Proterozoic-Archean zircons with peaks centered around 600 Ma, 1000 Ma, 2000 Ma, and 2650 Ma. The absence of Devonian-Precambrian age zircons in some bedrock samples (i.e., gneiss samples) is possibly due to the lithology of the samples (i.e., zircons from orthogneiss versus metasedimentary units).

New (n=3199) and published (n=1457) CSB and SB detrital zircon results (**Figure 6**) and new sandstone petrography results (**Figure 7**) characterize the provenance of sediment. The oldest CSB samples are Cenomanian to lower Campanian in age and are characterized by a major 76-110 Ma peak; few zircons are older than 110 Ma (n=22/660). These samples plot in the volcanic arc and recycled orogen fields. Samples younger than the lower Campanian have prominent Late Cretaceous (67-110 Ma) and Carboniferous (~325 Ma) peaks. The youngest CSB samples also contain a prominent Eocene peak (~41-58 Ma). About half of these samples have major or minor Triassic (~250 Ma), Devonian (375-400 Ma), and Proterozoic peaks around 600 Ma, 1000 Ma and 2000 Ma. The Sarıcakaya Basin samples have a similar distribution of DZ ages, yet for many SB samples, the pre-Cretaceous populations are more prevalent.

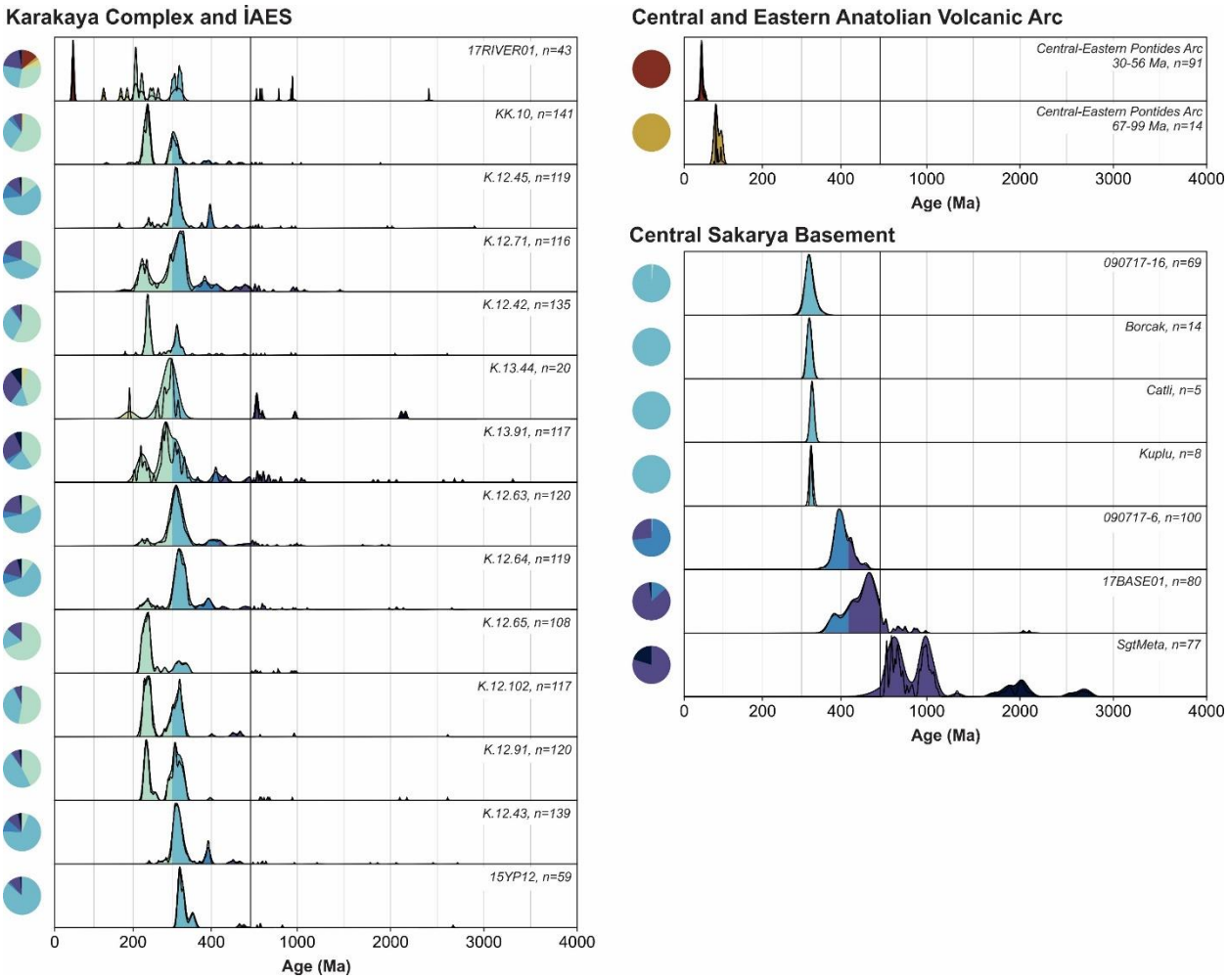

Figure 5. Detrital zircon age spectra characterizing potential sediment sources displayed probability density functions (black lines) and optimized fixed bandwidth kernel density estimates (black lines and shading). The Pontides volcanic arc ages are a compilation of pluton zircon U-Pb ages from the Central and Eastern Pontides. The Karakaya Complex samples are from Triassic sedimentary rocks and one modern river sample draining the İzmir-Ankara-Erzincan suture zone. The Central Sakarya Basement compilation includes bedrock and metasedimentary zircon U-Pb ages. See Figure 6 for color legend. Data sources: Campbell (2017); Mueller et al. (2019); Schleiffarth et al. (2018) and references therein; P. Ustaömer et al. (2012); T. Ustaömer et al. (2016); this study.

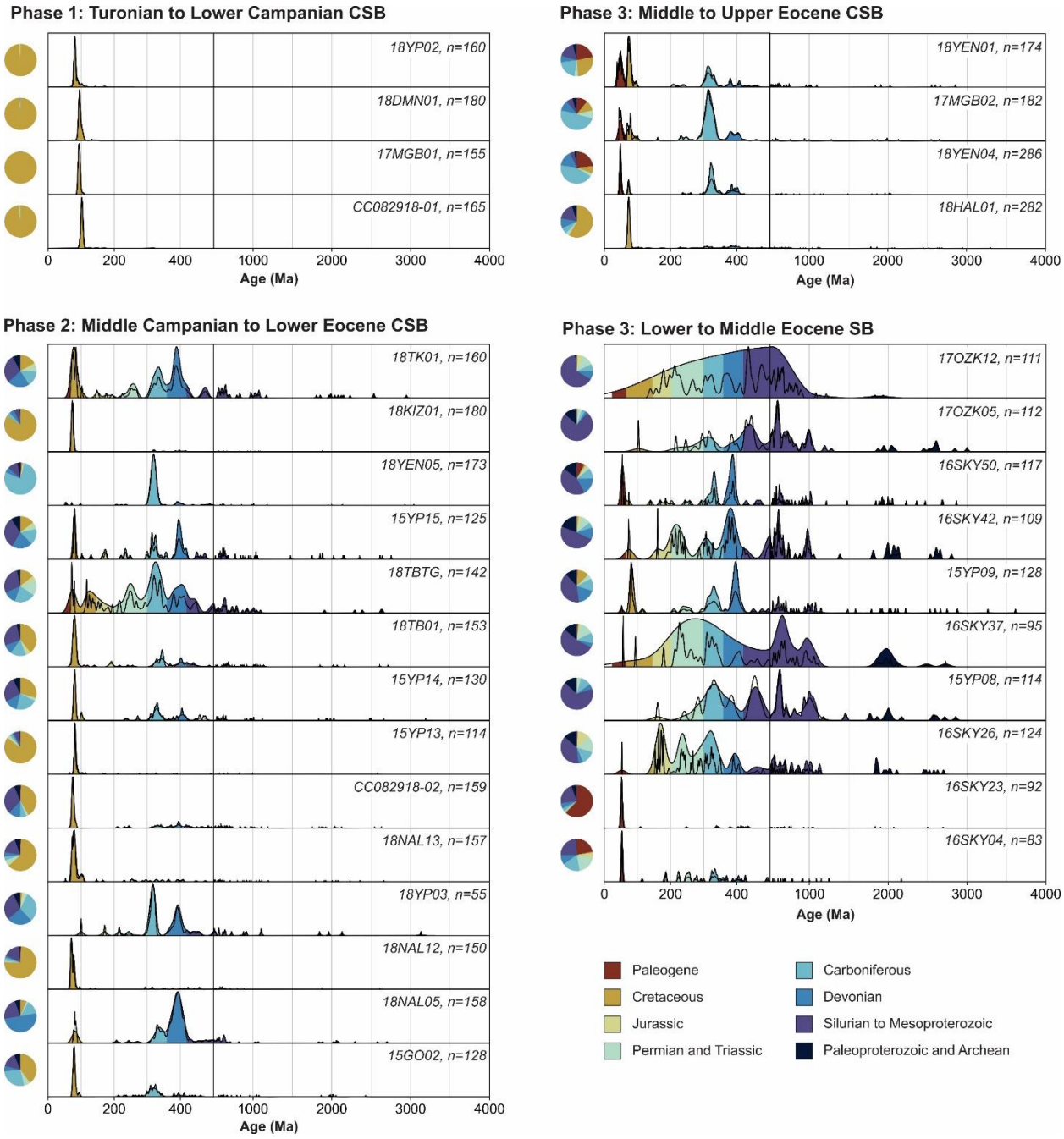

Figure 6. Detrital zircon age spectra from Central Sakarya Basin (CSB) and Sarıcakaya Basin (SB) detrital zircon samples grouped by Phase (see main text); Phase 3 is split into CSB and SB groups. Data are displayed as probability density functions (black lines) and optimized fixed bandwidth kernel density estimates (shaded black lines). Data sources: Campbell (2017); Mueller et al. (2019); Ocakoğlu et al. (2018); this study.

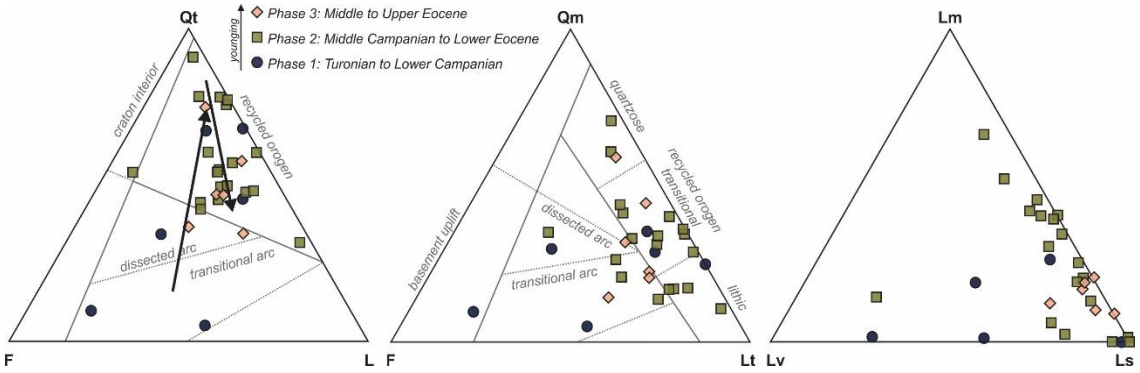

Figure 7. Ternary diagrams of sandstone modal composition from CSB. Samples are grouped by the sedimentary basin phases discussed in the text. Poles: Qt: total quartz; Qm: monocrystalline quartz; F: feldspar; L: lithics; Lm: metamorphic lithics; Ls: sedimentary lithics; Lv: volcanic lithics; Lt: total lithics (L + polycrystalline quartz).

5.2. Three Phases of the Central Sakarya Basin System

We subdivide the samples into three age groups based on major changes in DZ age distributions and sedimentary basin evolution (**Figure 8**). The sample ages, and therefore sample groups, are constrained in the CSB using published biostratigraphy, primarily planktonic foraminifera, and one tuff and one maximum depositional zircon U-Pb age (Ocakoğlu et al., 2018). The age of the SB samples is constrained by volcaniclastic U-Pb ages (Mueller et al., 2019). The new maximum depositional ages provided by our zircon age dataset do not add to the already-established chronological framework (Dataset S1).

Phase 1 includes Turonian through lower Campanian (94-76 Ma) DZ samples from the eastern CSB. This phase is characterized by a major 76-110 Ma peak; few zircons are older than 110 Ma (n=22/660) (**Figure 6** and **Figure 8**). Remnants of the Late Cretaceous volcanic arc are exposed along the present-day Black Sea southern coast, which is north of the CSB and Intra-Pontide Suture (**Figure 3;** Keskin & Tüysüz, 2018). However, pyroclastic flows, volcanogenic sandstones, and tuffs within the southern margin of the CSB are associated with Late Cretaceous submarine volcanism (Duru & Aksay, 2002; Gedik & Aksay, 2002; Ocakoğlu et al., 2018). Given the proximity to the submarine volcanism, the volcanic arc sediment compositions, and the

prevalence of Late Cretaceous zircon ages, Phase 1 strata are presumably first-cycle detritus derived from the nearby southern Late Cretaceous volcanic center within the CSB.

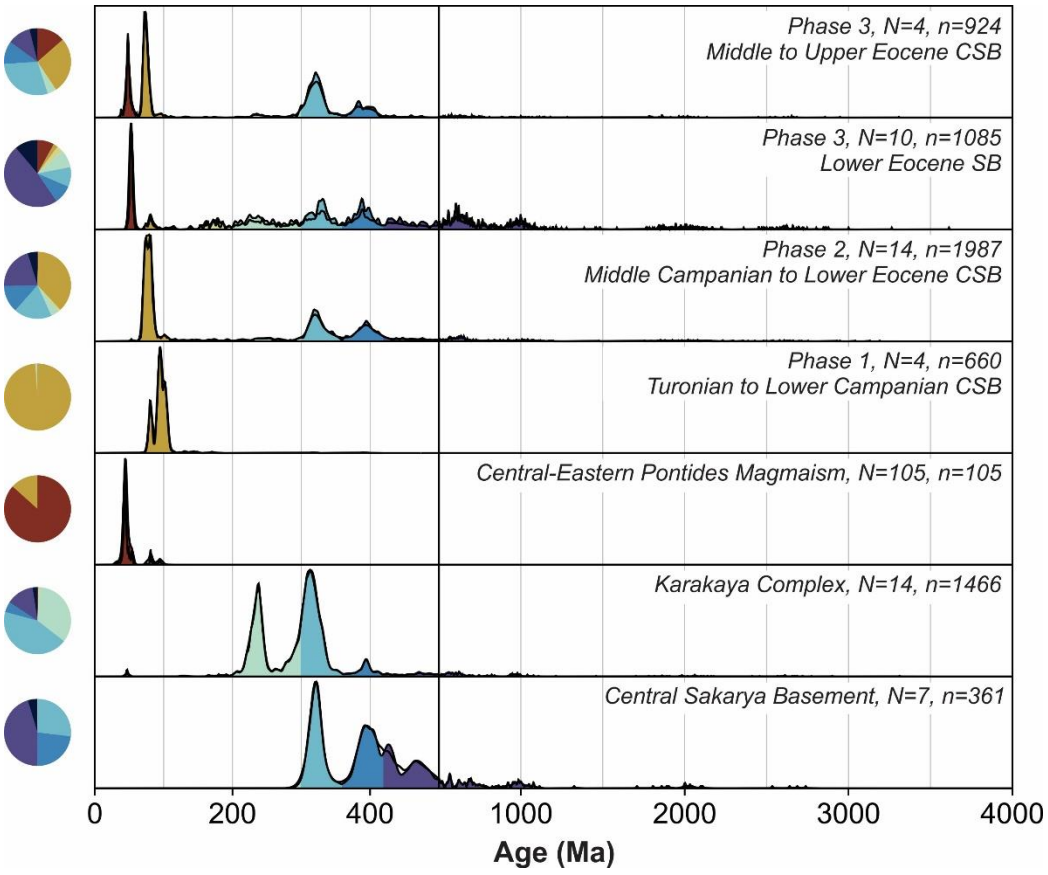

Figure 8. Probability density functions (black lines) and optimized fixed bandwidth kernel density estimates (black lines and shading) of all bedrock, modern, and detrital zircon ages grouped by basement terrane, basin, and stratigraphic age. See main text for discussion. Figure 6 contains the color legend.

Phase 2 includes middle Campanian through lower Eocene (76-54 Ma) samples. Phase 2 is defined by a major change in provenance with the appearance of basement-aged zircons (**Figure 8**), increased sedimentation rates (Ocakoğlu et al., 2018) and the onset of a lowstand systems tract (Ocakoğlu et al., 2007) around 76 Ma. In the Nallıhan section, the oldest samples in this phase fall between 77.61 Ma and 76.82 Ma based on planktonic foraminifera, and in the Göynük section the oldest Phase 2 sample has a published maximum depositional age of 76.4 ± 1.7 Ma based on the

youngest 19 zircons (Ocakoğlu et al., 2018). The middle Campanian through lower Eocene (76-54 Ma) sandstone compositions plot in the recycled orogen and volcanic arc fields. A trend of increasing quartz and sedimentary and metamorphic lithic compositions (**Figure 7**) coincides with the appearance of Paleozoic-Precambrian zircons. DZ samples are generally characterized by 67-90 Ma, 300-450 Ma and 550-700 Ma peaks. The presence of Carboniferous zircons alone or in tandem with Devonian and older zircons are either first-cycle zircons from Central Sakarya Basement or poly-cyclic zircons. The Central Sakarya Basement, containing Devonian and older zircon ages, was intruded by Variscan Carboniferous granitoids that are together exposed in the hanging wall of the Tuzaklı-Gümele Thrust (**Figure 2**). The exposures of Devonian through upper Neoproterozic plutons and crystalline basement rocks to the west and north of the CSB are an unlikely sediment source due to paleocurrent directions from the SW to NE and SE to NW (Ocakoğlu et al., 2018). The absence of Precambrian-aged zircons in most Central Sakarya Basement samples is likely due to sampling bias as most of the samples are orthogneiss and granitoids, with only one metasedimentary sample ('SgtMeta' from P. Ustaömer et al., 2012). The absence of deposition in the flexural SB before ~53 Ma indicates that the Tuzaklı-Gümele Thrust likely did not expose basement rocks in Phase 2. Therefore, during Phase 2, we propose that the basement-age zircons in the CSB appeared from sediment recycling during uplift and deformation of the southern margin of the Pontides. It is uncertain exactly where sediment recycling occurred or which structures were active, but it could be from the unroofing older sedimentary strata on the hanging wall of the Tuzaklı-Gümele Thrust.

Partitioning of the CSB by the basement-involved Tuzaklı-Gümele Thrust formed the broken-foreland SB. The Phase 2 to Phase 3 transition is defined by the onset of deposition in the SB, which is determined at 52.4 ± 0.6 Ma by volcaniclastic bed at the base of the Paleogene series in the SB (Campbell, 2017; Mueller et al., 2019). CSB sandstone compositions plot in the recycled orogen and volcanic arc fields, and lithics are predominantly sedimentary (**Figure 7**). Middle to upper Eocene (38-48 Ma) CSB samples are similar to those in Phase 2, with the addition of a 41-58 Ma peak. Eocene SB DZ samples are generally characterized by a 46-58 Ma peak along with 200-250 Ma, 325 Ma, 375-400 Ma, 600 Ma, 1000 Ma, 2000 Ma and 2600 Ma peaks. The increase in sedimentary lithics along with negligible changes in CSB DZ age spectra—except for the appearance of Eocene zircons—are consistent with continued sediment recycling and no major change in provenance.

The SB is interpreted as a flexural basin formed during partitioning of the CSB by the Tuzaklı-Gümele Thrust (Mueller et al., 2019). The SB received sediment from the Eocene volcanic arc, Karakaya Complex, and Central Sakarya Basement (**Figure 6** and **Figure 8**; Mueller et al., 2019). The SB is in the footwall of the Tuzaklı-Gümele Thrust; depositional environments, detrital zircon ages, and pebbles and boulders of quartz, mica and gneiss indicate that the Central Sakarya Basement was exposed in the hanging wall of the thrust by 52 Ma (Mueller et al., 2019). Therefore, the CSB received sediment from the hanging wall of the thrust, including recycled Phase 1 and Phase 2 deposits. The Eocene CSB samples contain Eocene zircons likely derived directly from Eocene volcanic and plutonic rocks located at the northern margin of the CSB or within the SB (**Figure 2 and Figure 3**). The Triassic and Carboniferous age doublet is distinctively Karakaya Complex in origin (**Figure 5**) and, given the absence of Triassic igneous rocks across Anatolia (**Figure 3**), the presence of this doublet indicates poly-cyclic zircons recycled from the Karakaya Complex. Only a few CSB samples received sediment from the Karakaya Complex (i.e., 18TBTG and 18TK01 from the Taraklı section in Phase 2), yet the Karakaya Complex is a prominent source to the Eocene SB samples. Therefore, sediment was likely sourced from exposed Karakaya Complex units near the suture zone into the nearby SB, and the absence of the Triassic-Carboniferous doublet in middle to upper Eocene CSB samples could point to disconnected CSB and SB depocenters. In addition, the scarcity of Silurian and older zircons in the middle to upper Eocene CSB samples could support disconnected drainage networks.

6. Evolution of the Central Sakarya Basin in Context

All CSB and SB DZ ages from 150 to 30 Ma are combined and plotted alongside simplified composite stratigraphic columns (**Figure 9**). We interpret the combined DZ ages from 150 to 30 Ma as the magmatic arc tempo of the Anatolian arc (Paterson & Ducea, 2015). The apparent magmatic lulls at 67-58 Ma and starting at 41 Ma are consistent with the 72-58 Ma and 40-20 Ma magmatic lulls in central and eastern Anatolia based on a compilation of 100-0 Ma bedrock crystallization and cooling ages (Schleiffarth et al., 2018).

We discuss the three major provenance phases in terms of basin evolution. During Phase 1 (94-76 Ma), the Late Cretaceous volcanic arc, located within the CSB (Gedik & Aksay, 2002; Ocakoğlu et al., 2018) and along the southern Black Sea coast (Keskin & Tüysüz, 2018), was the dominant source of sediment to the forearc CSB (**Figure 6**; Yilmaz et al., 2010). This 34 Myr

phase is not associated with any change in depositional style, accumulation rate (Ocakoğlu et al., 2018) or provenance (**Figure 6** and **Figure 7**). This period corresponds to a standard Andean-type active margin setting with a phase of Santonian-Campanian extension (Ocakoğlu et al., 2018). The brief magmatic lull at 88 Ma (**Figure 9)** could be the signal of pre-collisional TVZ subduction.

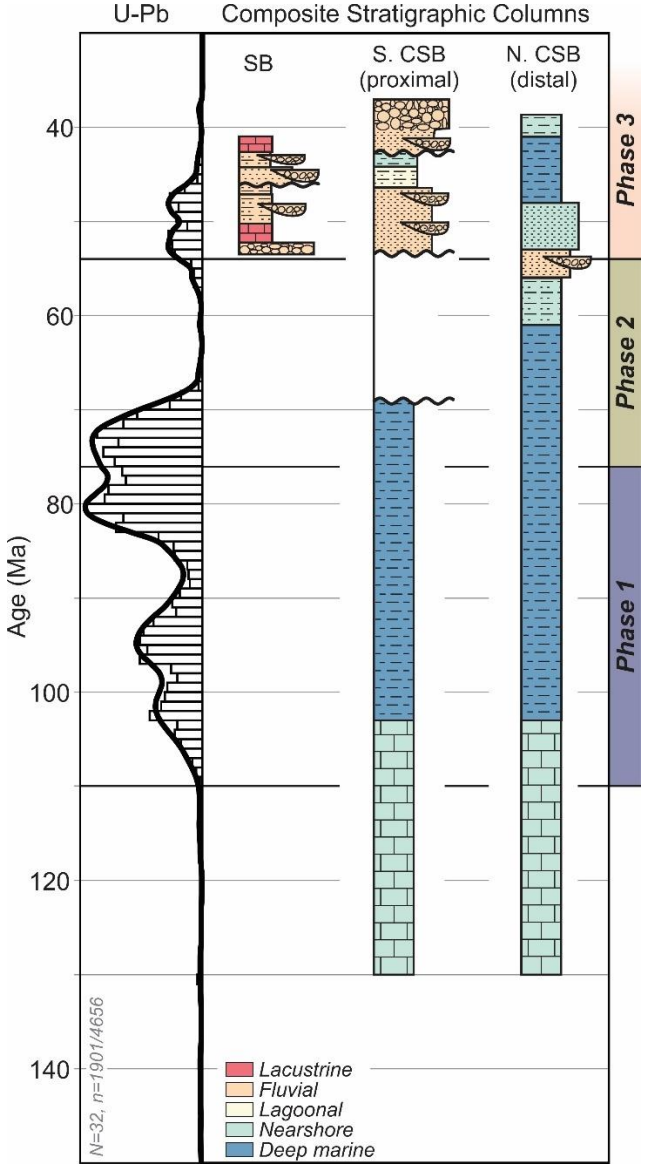

Figure 9. Combined detrital zircon U-Pb results alongside stratigraphic columns. All detrital zircon ages from 150 to 30 Ma from a compilation of all SB and CSB samples are displayed as a histogram (1 Myr bin) and probability density function. The CSB and SB composite stratigraphic columns are after Ocakoğlu et al. (2018) and Mueller et al. (2019), respectively (see **Figure 4**). Shading highlights the three sedimentary basin phases discussed in the text.

433

434 During Phase 2 (76-54 Ma), CSB strata are characterized by DZ ages typical of Pontide
435 basement units (**Figure 8**; P. Ustaömer et al., 2012) and evolve toward quartz- and sedimentary
436 lithic-rich compositions suggesting an unroofing sequence in which poly-cyclic basement-aged
437 zircons appeared in the basin. Input of ophiolitic material into the CSB starting at ca. 73 Ma, as
438 shown by increased mafic/felsic element ratios (i.e., Ni/Zr, Ni/Y, Cr/Zr) in the distal İsmailler
439 section (Açıkalın et al., 2016), pinpoint the area of exhumation to the İAES where ophiolitic units
440 and the Karakaya Complex are exposed today. Flute casts and asymmetrical ripples record
441 paleocurrent directions indicating flow toward the NE-NW (Ocakoğlu et al., 2018). Together this
442 indicates that the southern margin of the SKZ, including the İAES accretionary complex, began
443 uplifting, exhuming, and creating south-to-north flowing, transverse drainage systems in the
444 southern CSB at 76 Ma. Arc shutdown and initial underthrusting is contemporaneous with the
445 slowing of convergence rates from 28 mm/yr at 110-76 Ma to 5 mm/yr from 76 Ma onwards (rates
446 calculated from plate reconstructions based on paleomagnetic and kinematic data in van
447 Hinsbergen et al., 2020). Evolved εHf values in Late Cretaceous zircons indicate either crustal
448 thickening, lower plate continental underthrusting, or arc migration into evolved continental crust;
449 we favor lower plate underthrusting due to the coeval decrease in magmatic tempo (**Figure 9**).
450 Exhumation and underthrusting continued, recorded as the onset of northward prograding deltas
451 at 61 Ma, development of a major unconformity in the proximal (southern) CSB, transition from
452 flysch to molasse, and an order of magnitude increase in CSB accumulation rates (Açıkalın et al.,
453 2016; Ocakoğlu et al., 2018). These CSB changes coincide with a 67-58 Ma magmatic lull (**Figure**
454 **6**), and 63-57 Ma TVZ Barrovian metamorphism to greenschist and amphibolite facies (e.g.,
455 Whitney et al., 2011) and subsequent 60 Ma exhumation as indicated by white mica $^{40}Ar/^{39}Ar$
456 cooling ages (Seaton et al., 2009).

457 The Phase 2 to Phase 3 transition (~54 Ma) is marked by the onset of deposition in the SB
458 by 52.4 Ma (Mueller et al., 2019) and partitioning of the CSB by the basement-involved Tuzaklı-
459 Gümele Thrust. Basin partitioning is coeval with the resumption of deposition in the southern CSB
460 and the transition to continental facies and prograding clastic wedges in the CSB sometime around
461 58-54 Ma (Ocakoğlu et al., 2018). There was continued sediment recycling and no significant
462 provenance change in the CSB (**Figure 5** and **Figure 7**). Deformation and exhumation propagated
463 north of the İAES; basement-involved shortening (Şahin et al., 2019) structurally partitioned the

SB and CSB foreland along the lithospheric-scale Karakaya Complex–Central Sakarya Basement boundary (Tuzaklı-Gümele Thrust in **Figure 2**; Mueller et al., 2019). The difference in Precambrian zircon abundance between the CSB and SB likely indicates fully disconnected basin depocenters (**Figure 8**). This phase is coeval with linear belts of Eocene magmatism (58-41 Ma) along the İAES and Intra-Pontide suture zones (Altunkaynak, 2007; Altunkaynak et al., 2012; Dilek & Altunkaynak, 2009; Ersoy, Akal, et al., 2017; Ersoy, Palmer, et al., 2017; Harris et al., 1994; Kasapoğlu et al., 2016; Okay & Satir, 2006; Yildiz et al., 2015). Seaways persisted into Phase 3 as indicated by Lutetian-Priabonian marine deposition in the distal (northern) CSB (e.g., Ocakoğlu et al., 2018), which suggests there was not significant regional surface uplift during Phase 3.

7. Implications for Geodynamic Mechanisms Controlling Collisional Deformation

This section explores the possible geodynamic mechanisms that could explain a ~20 Myr multi-phase collision along the İAES. Multi-phased, "soft-hard" collisions have been proposed numerous times in the Tethyan domain (e.g., Ballato et al., 2018; Beaumont et al., 1996; Darin et al., 2018; Jagoutz et al., 2016; Kaymakci et al., 2009; Pourteau et al., 2016; Tye et al., 2020) and worldwide. These scenarios are based on a variety of mechanisms: subduction of a highly extended lower plate oceanic and continental lithosphere (van Hinsbergen et al., 2011, 2012), arc-continent collision (Jagoutz et al., 2016; Martin et al., 2020), upper plate pre-existing structures and sediment thickness (Jones et al., 1998, 2011; Parker & Pearson, 2021), slab breakoff (DeCelles et al., 2011; Sinclair, 1997), relict basin closure (Cowgill et al., 2016), and increased lower plate lithospheric thickness (Ballato et al., 2011; Soret et al., 2021). One or a combination of these scenarios could explain the protracted nature of intercontinental collision in western Anatolia, including the thick-skinned deformation and basin partitioning at 54 Ma.

Several mechanisms for protracted Tethyan collisions are not applicable in western Anatolia. For the collision of India with Asia, discrepancies between shortening and convergence led to several geodynamic mechanisms for protracted and multi-stage collision (e.g., Hu et al., 2016; Kapp & DeCelles, 2019 and references therein), such as a wide lower plate lithosphere (i.e., Greater India; van Hinsbergen et al., 2011, 2012) and initial collision of an intra-oceanic arc (Jagoutz et al., 2015, 2016; Martin et al., 2020). While there likely was a wide pre-collisional lower plate TVZ lithosphere and possibly an intra-oceanic arc (Göncüoğlu et al., 2000, 2010;

Sarıfakıoğlu et al., 2009, 2017), the most recent plate reconstructions require only a few hundred kilometers between the SKZ and TVZ in the early Campanian (van Hinsbergen et al., 2020). Therefore, these mechanisms that explain thousands of kilometers of distance between continental domains and shortening deficits during initial collisional deformation are not applicable in western Anatolia. Furthermore, upper plate conditions, such as those proposed for the North American Cordillera (i.e., sediment thickness, pre-existing structures, cratonic keel; e.g., Jones et al., 1998, 2011; Parker & Pearson, 2021), could control the activation of the thick-skinned Tuzaklı-Gümele Thrust, which could be the reactivation of the boundary between the accreted Karakaya Complex and the SKZ crystalline basement. Yet, unlike the North American Cordillera, there is not evidence that the style of deformation is caused by the pre-deformational stratigraphic thickness (i.e., mechanical stratigraphic control in Parker & Pearson, 2021). In the remaining part of the discussion, we focus on the three mechanisms that we think are the most viable for the İAES closure.

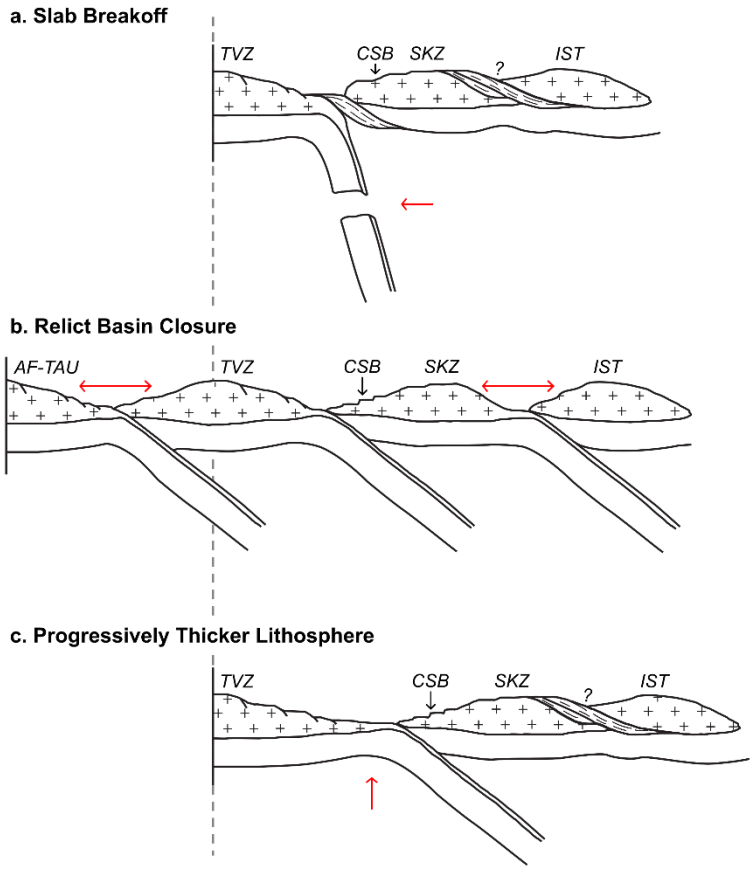

Figure 10. Schematic diagram of multi-phase collision scenarios (inspired by Darin et al., 2018; Di Rosa et al., 2019; Göncüoğlu et al., 2014). (**a**) Tavşanlı Zone slab breakoff. (**b**) Relict basin closure between the Sakarya (SKZ) and Istanbul (IST) Zones in the north and/or the Tavşanlı Zone (TVZ) and Afyon Zone or Tauride terrane (AF-TAU) in the south (see Figure 1). (**c**) Subduction and underthrusting of progressively thicker Tavşanlı Zone continental lithosphere.

524

525

526 7.1. Slab Breakoff

527 Slab breakoff is a mechanism commonly employed to explain coeval surface uplift,
528 extension and magmatism (von Blanckenburg & Davies, 1995; Davies & von Blanckenburg,
529 1995), although its prevalence in the geologic past and connection to magmatism is questioned
530 (Garzanti et al., 2018; Niu, 2017). In western Anatolia, slab breakoff can explain the timing and
531 geochemical signature of ~58-40 Ma magmatism (Altunkaynak et al., 2012; Dilek & Altunkaynak,
532 2009; Ersoy, Akal, et al., 2017; Ersoy, Palmer, et al., 2017; Harris et al., 1994; Kasapoğlu et al.,
533 2016). However this interpretation is debated (P. Ustaömer et al., 2009; see also Mueller et al.,
534 2019; Okay & Whitney, 2010; Okay & Satir, 2006; van Hinsbergen et al., 2010) for four main
535 reasons: (1) the TVZ slab was subducted to mantle depths in the Late Cretaceous and the
536 exhumation of blueschists in the Campanian-Maastrichtian suggests slab breakoff was in the Late
537 Cretaceous not Eocene (e.g., Okay & Satir, 2006); (2) geodynamic models of slab breakoff predict
538 >1.5 km of surface uplift across several hundreds of kilometers across-strike (Göğüş et al., 2016).
539 Yet, across the <150 km İAES and CSB (**Figure 2**), Paleocene-Eocene marine deposition in the
540 CSB indicates there was not significant uplift; (3) there was early Eocene contractional
541 deformation in the SB and no evidence for extension (Mueller et al., 2019; Şahin et al., 2019); (4)
542 magmatism was contemporaneous across three parallel volcano-plutonic belts at the northern
543 margin of the CSB, bisecting the SB, and in the TVZ (**Figure 3**; e.g., Ersoy, Akal, et al., 2017;
544 Ersoy, Palmer, et al., 2017; Harris et al., 1994; Kasapoğlu et al., 2016). Slab breakoff has been
545 inferred in extensional sedimentary basins based on the observation of alternating clastic and
546 lacustrine deposits, an overall fining-upward sedimentary succession, high sedimentation rates,
547 and an absence of contractional growth structures in extensional basins are interpreted as the result
548 of slab breakoff (DeCelles et al., 2011; Leary et al., 2016). Although the SB contains alternating
549 clastic floodplain and lacustrine limestone deposits and no contractional growth strata, clasts of
550 quartz, mica and gneiss in coarse-grained fluvial deposits along with the presence of basement-
551 aged zircons indicates that the basement-involved Tuzaklı-Gümele Thrust was active in the early
552 Eocene (Mueller et al., 2019). Geodynamic explanations for Eocene magmatism remain
553 inconclusive; alternative arguments include lithospheric delamination (van Hinsbergen et al.,

2010; Pourteau et al., 2013), arc volcanism from a different subduction zone system (Okay & Satir, 2006), and mid-to-late Eocene orogenic collapse and extension (P. Ustaömer et al., 2009). Despite these numerous limitations, the slab break-off model remains a popular mechanism. We note that an amagmatic slab breakoff (Garzanti et al., 2018; Niu, 2017) occurring ~10 Myr after initial collision, during the 67-58 Ma magmatic lull and Yenipazar section angular unconformity, could partly solve these issues and provide a mechanism to delay contractional deformation and juvenile magmatism (**Figure 10a**).

7.2. Relict Basin Closure

Although slightly different in nature, in both the Arabia-Eurasia and India-Asia collisions, the initial collision of upper plate island arcs or continental terranes with the lower plate continental lithosphere results in upper plate backarc basin closure (e.g., Cowgill et al., 2016; Jagoutz et al., 2015; Kapp & DeCelles, 2019). Initial Arabian collision is inferred from the coeval ca. 36 Ma magmatic lull and switch in kinematic regime from extensional to contractional in the Alborz Mountains of Iran (Ballato et al., 2011), and increased exhumation rates in the eastern Taurides (Darin et al., 2018) and in the central Pontides (Ballato et al., 2018). Yet initial foreland basin sedimentation (Ballato et al., 2011), slowed convergence rates (McQuarrie et al., 2003), increased exhumation near the Bitlis suture zone (Okay et al., 2010) was delayed until at 20-17 Ma. Cowgill et al. (2016) suggest that significant upper plate deformation from the Arabia-Eurasia collision was delayed by ~15-20 Myr by northward jumping deformation. In this scenario, collisional stress was transferred through the lithosphere and closed several upper plate basins (Cowgill et al., 2016). Eocene-Oligocene Arabian collision along the Bitlis-Zagros suture (e.g., Koshnaw et al., 2019; McQuarrie et al., 2003; McQuarrie & van Hinsbergen, 2013) initiated backarc basin subduction between the Lesser and Greater Caucasus (e.g., Avdeev & Niemi, 2011); then, basin closure around 5 Ma produced a 10-fold increase in Greater Caucasus exhumation rates (Avdeev & Niemi, 2011) coincident with foreland basin erosion and non-deposition, mixing of sediment from the upper and lower plates, and provenance signatures of progressive crustal exhuming (e.g., Tye et al., 2020).

In line with this relict basin closure scenario, major collisional deformation from initial TVZ-SKZ underthrusting could be delayed by >20 Myr due to the closure of relict basins to the north or south of the İAES (**Figure 10b**). The closure of the Intra-Pontide suture zone is a strong

584 candidate to explain this delay because the timing of suturing remains unclear, with proposed ages
585 spanning from the Early Cretaceous (Akbayram et al., 2013), Late Cretaceous-Paleocene (Di Rosa
586 et al., 2019; Göncüoğlu et al., 2000; Z. Özcan et al., 2012; Robertson & Ustaömer, 2004) to the
587 Paleocene-Eocene (Akbayram et al., 2016; Göncüoğlu et al., 2014; Okay et al., 1994). Major
588 contractional deformation could also be delayed by the hypothesized southward-jumping
589 subduction zones synchronously or sequentially facilitating the closure of Neotethyan oceanic
590 basins between Anatolide and Tauride terranes south of the İAES (Pourteau et al., 2013, 2016).
591 Resumed or increased continental underthrusting at 54 Ma along the İAES could partly explain
592 the renewal of magmatism without explaining its regional distribution. The lack of consensus on
593 the history of Intra-Pontide rifting and suturing makes it difficult to estimate the applicability of
594 this mechanism.

595 7.3. Increasing Lithospheric Thickness of the Lower Plate

596 An alternate two-stage collision scenario, also invoked for Tethyan collisions, involves the
597 gradual increase in thickness of underthrusting lower plate lithosphere (e.g., Ballato et al., 2011;
598 Darin et al., 2018; Soret et al., 2021). In the Himalayan sector, the initial collision of India with
599 Asia is generally accepted to be 60-55 Ma, when the final vestiges of Neotehyan oceanic crust
600 were subducted (Hu et al., 2016 and references therein). In northern Pakistan, Barrovian
601 metamorphism from 47 to 38 Ma is coincident with the formation and exhumation of eclogites
602 (Soret et al., 2021) along with a >50% decrease in convergence rates at 50-45 Ma (van Hinsbergen
603 et al., 2011) and increased exhumation in the Himalaya starting around 35 Ma (Ding et al., 2016).
604 Soret et al. (2021) suggest that initial collision, as defined by oceanic basin closure, was followed
605 by a phase of "continental subduction" when there was Barrovian metamorphism and convergence
606 was accommodated by underplating and tectonic stacking during the slow underthrusting of
607 thinned passive margin lithosphere beneath Asia. Then, "collisional initiation" began ca. 38 Ma
608 when increased mechanical coupling between India and Asia significantly increased thrust faulting
609 (i.e., Main Mantle thrust, Karakorum fault), exhumation, uplift and erosion rates (Soret et al.,
610 2021).

611 Therefore, multi-phase collision in western Anatolia could be attributed to the arrival of
612 progressively thicker, buoyant TVZ continental lithosphere beneath the SKZ (**Figure 10c**). At 76
613 Ma, the initial "soft" collision, or "continental subduction," involving thin passive margin

lithosphere locked the subduction zone megathrust and triggered upper plate shortening (Beaumont et al., 1996; Tye et al., 2020). The appearance of basement-aged zircons in the CSB at 76 Ma is closely followed by a regional unconformity (Ocakoğlu et al., 2007), magmatic lull (67-58 Ma), TVZ Barrovian metamorphism (63-57 Ma; e.g., Whitney et al., 2011), and TVZ exhumation (60 Ma; Seaton et al., 2009). Subsequent thick-skinned deformation and basin partitioning by 54 Ma (Mueller et al., 2019; Şahin et al., 2019) would represent the final "hard" collision, or "collisional initiation," defined by the arrival of full-thickness continental lithosphere along the subduction zone and a more substantial plate coupling manifested as widespread regional contractional deformation. A convergence rate of ~5 mm/yr from 76 to 54 Ma (van Hinsbergen et al., 2020) predicts 110 km of TVZ underthrusting, which is less than estimates for the amount of underthrust thinned, passive margin Arabian lithosphere (~400-480 km; Ballato et al., 2011; Darin et al., 2018). Therefore, this mechanism is feasible to explain the collisional evolution of the İAES in western Anatolia.

7.4. Geodynamic Influence on Mediterranean Biogeography

Even though it remains difficult to pinpoint a specific mechanism for protracted collision and delay in upper plate deformation, our results highlight a direct—and unexpected—geodynamic and paleogeographic control on the regional fauna. Backarc rifting in the middle Cretaceous isolated the Pontides from Eurasia (Akdoğan et al., 2019; Okay & Nikishin, 2015), setting the stage for Paleogene endemism. In Cretaceous-Paleogene times, Anatolia was an island archipelago separated from large continental domains (i.e., Afro-Arabia, Europe and Asia) by strands of the Paleotethys and Neotethys oceans (Barrier & Vrielynck, 2008; van Hinsbergen et al., 2020). Gradual Late Cretaceous to early Eocene İAES suture zone formation favored colonization of the Pontides by Gondwanan and Laurasian mammalian clades via "island hopping" across the Neotethyan archipelago (Beard et al., 2020; Jones et al., 2018; Kappelman et al., 1996; Licht et al., 2017; Métais et al., 2017; Sen, 2013). The TVZ-SKZ collision assembled a larger subaerial continental landmass that further promoted *in situ* diversification of endemic taxa (Maas et al., 2001; Métais et al., 2018). Endemism persisted until at least the Lutetian (44-43 Ma; Licht et al., 2017), a time when much of Anatolia was near sea level—many sedimentary basins record a Lutetian marine incursion (e.g., Licht et al., 2017; Lygina et al., 2016; MTA, 2002; Ocakoğlu et al., 2012; E. Özcan et al., 2019; Racey, 2001). Therefore, the protracted nature of the collision

might explain the persistence of seaways and faunal isolation until late in the collision timeline (Beard et al., 2020b; M. F. Jones et al., 2018; Licht et al., 2017; Métais et al., 2018; Sen, 2013). In this way, the protracted nature of İAES collision is relevant to the evolution of emergent landmasses and exemplifies a direct influence of geodynamics and tectonics on biogeography.

8. Conclusion

Our results from one sedimentary basin system indicate that discrepancies among proxies of collision age are not an artifact of different geologic datasets or along strike variability, but instead can be reconciled by a multi-stage TVZ-SKZ collision in western Anatolia. The first step of Neotethyan closure (94-76 Ma) is during the obduction of Neotethyan ophiolites on the TVZ at ca. 95 Ma (e.g., Okay & Whitney, 2010; Robertson et al., 2009) and backarc spreading (i.e., Black Sea basin) that separated the Pontides from the Eurasian margin, thus highlighting that extension rather than shortening dominated upper plate dynamics (Okay et al., 2013; Okay and Nikishin, 2015; Ocakoğlu et al., 2018). During this time, the CSB forearc basin received detritus from the Pontide volcanic arc, likely located at the southern margin of the CSB. TVZ subduction and subsequent exhumation is not associated with any changes in sedimentary provenance in the forearc CSB, confirming that TVZ subduction occurred far offshore the SKZ margin (at ca. 750 km based on calculations from the plate reconstructions in van Hinsbergen et al. (2020)) in an intra-oceanic subduction zone (Göncüoğlu et al., 2000, 2010; Sarıfakıoğlu et al., 2009, 2017). Phase 2 started at 76 Ma with the appearance of basement-derived zircons in CSB strata followed by the onset of northward prograding deltas and increased in mafic input (Açıkalın et al., 2016; Ocakoğlu et al., 2018; this study). These results all highlight an onset of İAES uplift and exhumation and indicate a switch in deformation regime at the southern margin of the basin with the start of thick-skinned deformation. These events are coeval to a regional arc shutdown and are thus attributed to the onset of TVZ-SKZ continental collision and the beginning of TVZ underthrusting below SKZ. Phase 3 began at 54 Ma and is associated with a shift from thin- to thick-skinned thrusting, foreland basin partitioning, and regional syn-collisional magmatism. This shift in deformation regime 20 Myr after initial intercontinental collision emphasizes the protracted nature of the collision.

The structural complexity of the Anatolian lithosphere with numerous tectonic units and sutures calls for a polygenetic evolution. The timing İAES closure and duration of suturing may

be explained best by aspects of three multi-phase collision models: slab breakoff, relict basin closure, and subduction of progressively thicker lithosphere. Each of these models predicts a change in plate coupling that can explain the 20 Myr delay between initial intercontinental collision and thick-skinned deformation. Given the debated chronology of Intra-Pontide suturing and Eocene magmatism, the subduction of progressively thicker lithosphere remains the best and simplest explanation for protracted collision in western Anatolia. The uninterrupted sedimentary record of the forearc-to-foreland Central Sakarya Basin records a complete history of progressive intercontinental collision that can serve as an example for Tethyan collisions. This sedimentary basin highlights how the 15-40 Myr discrepancies of collision age across the Alpine-Himalayan belt can be reconciled and synthesized into a holistic model for protracted collisions with geodynamic mechanisms involving changing plate coupling.

Acknowledgments

We thank Cassandra Brigham, Alison Duvall, Katharine Huntington, Begüm Kurtoğlu, Spencer Mattingly, Çelik Ocakoğlu, Ben Paulson, Aurora Rosenberger, Theresa Schwartz, Tamas Ugrai, and Melissa Wood for prolific discussions and for field and lab assistance. We thank Editor Peter van der Beek and two anonymous reviewers for improving the manuscript. This work was supported by NSF EAR-1543684. Datasets for this research are included in the supplementary information files and archived in a Mendeley data repository (link to be included here upon publication).

see ESSOAr supplemental files:

Table 1. New and published samples, units, ages, groups, sample types, and sources. See Figure 2 for sample locations. DZ: detrital zircon; SP: sandstone petrography. Data sources: 1: P. Ustaömer et al., 2012, 2: T. Ustaömer 2016; 3: Campbell, 2017; 4: Ocakoğlu et al., 2018; 5: Schleiffarth et al., 2018 and references therein; 6: Mueller et al., 2019; 7: this study.

9. References

Açıkalın, S., Ocakoğlu, F., Yılmaz, İ. Ö., Vonhof, H., Hakyemez, A., & Smit, J. (2016). Stable isotopes and geochemistry of a Campanian–Maastrichtian pelagic succession, Mudurnu–Göynük Basin, NW Turkey: Implications for palaeoceanography, palaeoclimate and sea-level fluctuations. *Palaeogeography, Palaeoclimatology, Palaeoecology*, *441*, 453–466. https://doi.org/10.1016/j.palaeo.2015.10.005

Akbayram, K., Okay, A. I., & Satır, M. (2013). Early Cretaceous closure of the Intra-Pontide Ocean in western Pontides (northwestern Turkey). *Journal of Geodynamics*, *65*, 38–55. https://doi.org/10.1016/j.jog.2012.05.003

Akbayram, K., Sengor, A. M. C., & Ozcan, E. (2016). The evolution of the intra-Pontide suture; implications of the discovery of late Cretaceous-early Tertiary melanges. *Geological Society of America, Special Paper 525*. https://doi.org/10.1130/2016.2525(18)

Akdoğan, R., Okay, A. I., Sunal, G., Tari, G., Meinhold, G., & Kylander-Clark, A. R. C. (2017). Provenance of a large Lower Cretaceous turbidite submarine fan complex on the active Laurasian margin: Central Pontides, northern Turkey. *Journal of Asian Earth Sciences*, *134*, 309–329. https://doi.org/10.1016/j.jseaes.2016.11.028

Akdoğan, R., Okay, A. I., & Dunkl, I. (2019). Striking Variation in the Provenance of the Lower and Upper Cretaceous Turbidites in the Central Pontides (Northern Turkey) Related to the Opening of the Black Sea. *Tectonics*, *38*(3), 1050–1069. https://doi.org/10.1029/2018TC005119

Aksay, A., Pehlivan, Ş., Gedik, I., Bılginer, E., Duru, M., Akbaş, B., & Altun, I. (2002). Geologic map of Turkey (Zonguldak, Scale 1:500,000). Ankara, Turkey: Maden Tetkik ve Arma Genel Müdürlüğü.

Altiner, D., Kocyigit, A., Farinacci, A., Nicosia, U., & Conti, M. A. (1991). Jurrasic-Lower Cretaceous stratigraphy and paleogeographic evolution of the southern part of North-Western Anatolia (Turkey). *Geologica Romana*, *27*, 13–80.

Altunkaynak, Ş. (2007). Collision-Driven Slab Breakoff Magmatism in Northwestern Anatolia, Turkey. *The Journal of Geology*, *115*(1), 63–82. https://doi.org/10.1086/509268

Altunkaynak, Ş., Sunal, G., Aldanmaz, E., Genç, C. Ş., Dilek, Y., Furnes, H., et al. (2012). Eocene Granitic Magmatism in NW Anatolia (Turkey) revisited: New implications from comparative zircon SHRIMP U–Pb and 40Ar–39Ar geochronology and isotope geochemistry on magma genesis and emplacement. *Lithos*, *155*, 289–309. https://doi.org/10.1016/j.lithos.2012.09.008

Alvarez, W. (2010). Protracted continental collisions argue for continental plates driven by basal traction. *Earth and Planetary Science Letters*, *296*(3), 434–442. https://doi.org/10.1016/j.epsl.2010.05.030

Avdeev, B., & Niemi, N. A. (2011). Rapid Pliocene exhumation of the central Greater Caucasus constrained by low-temperature thermochronometry. *Tectonics*, *30*(2). https://doi.org/10.1029/2010TC002808

Ballato, P., Uba, C. E., Landgraf, A., Strecker, M. R., Sudo, M., Stockli, D. F., et al. (2011). Arabia-Eurasia continental collision: Insights from late Tertiary foreland-basin evolution in the Alborz Mountains, northern Iran. *GSA Bulletin*, *123*(1–2), 106–131. https://doi.org/10.1130/B30091.1

Ballato, P., Parra, M., Schildgen, T. F., Dunkl, I., Yıldırım, C., Özsayın, E., et al. (2018). Multiple Exhumation Phases in the Central Pontides (N Turkey): New Temporal Constraints on Major Geodynamic Changes Associated With the Closure of the Neo-Tethys Ocean. *Tectonics*, *37*(6), 1831–1857. https://doi.org/10.1029/2017TC004808

Barrier, E., & Vrielynck, B. (2008). *Palaeotectonic Maps of the Middle East*. Paris.

Baş, H. (1986). Tertiary geology of the Domaniç-Tavsanli-Kütahya-Gediz Region. *Jeoloji Mühendisliği*, *27*(11), 11–18.

Beard, K. C., Métais, G., Ocakoğlu, F., & Licht, A. (2020a). An omomyid primate from the Pontide microcontinent of north-central Anatolia: Implications for sweepstakes dispersal of terrestrial mammals during the Eocene. *Geobios*. https://doi.org/10.1016/j.geobios.2020.06.008

Beard, K. C., Métais, G., Ocakoğlu, F., & Licht, A. (2020b). An omomyid primate from the Pontide microcontinent of north-central Anatolia: Implications for sweepstakes dispersal of terrestrial mammals during the Eocene. *Geobios*. https://doi.org/10.1016/j.geobios.2020.06.008

Beaumont, C., Ellis, S., Hamilton, J., & Fullsack, P. (1996). Mechanical model for subduction-collision tectonics of Alpine-type compressional orogens. *Geology*, *24*(8), 675–678. https://doi.org/10.1130/0091-7613(1996)024<0675:MMFSCT>2.3.CO;2

Becker, T. W., & Faccenna, C. (2011). Mantle conveyor beneath the Tethyan collisional belt. *Earth and Planetary Science Letters*, *310*(3), 453–461. https://doi.org/10.1016/j.epsl.2011.08.021

von Blanckenburg, F., & Davies, J. H. (1995). Slab breakoff: A model for syncollisional magmatism and tectonics in the Alps. *Tectonics*, *14*(1), 120–131. https://doi.org/10.1029/94TC02051

Campbell, C. F. (2017). *Tectonic Evolution of the Izmir-Ankara Suture Zone in Northwest Turkey using Zircon U-Pb Geochronology and Zircon Lu-Hf Isotopic Tracers* (M.S.). University of Kansas, United States -- Kansas. Retrieved from http://search.proquest.com/pqdtglobal/docview/2019635859/abstract/4D50BF261D204844PQ/1

Cowgill, E., Forte, A. M., Niemi, N., Avdeev, B., Tye, A., Trexler, C., et al. (2016). Relict basin closure and crustal shortening budgets during continental collision: An example from Caucasus sediment provenance. *Tectonics*, *35*(12), 2918–2947. https://doi.org/10.1002/2016TC004295

Darin, M. H., Umhoefer, P. J., & Thomson, S. N. (2018). Rapid Late Eocene Exhumation of the Sivas Basin (Central Anatolia) Driven by Initial Arabia-Eurasia Collision. *Tectonics*. https://doi.org/10.1029/2017TC004954

Davies, J. H., & von Blanckenburg, F. (1995). Slab breakoff: A model of lithosphere detachment and its test in the magmatism and deformation of collisional orogens. *Earth and Planetary Science Letters*, *129*(1), 85–102. https://doi.org/10.1016/0012-821X(94)00237-S

DeCelles, P. G., Kapp, P., Quade, J., & Gehrels, G. E. (2011). Oligocene–Miocene Kailas basin, southwestern Tibet: Record of postcollisional upper-plate extension in the Indus-Yarlung suture zone. *GSA Bulletin*, *123*(7–8), 1337–1362. https://doi.org/10.1130/B30258.1

Di Rosa, M., Farina, F., Marroni, M., Pandolfi, L., Göncüoğlu, M. C., Ellero, A., & Ottria, G. (2019). U-Pb zircon geochronology of intrusive rocks from an exotic block in the Late Cretaceous – Paleocene Taraklı Flysch (northern Turkey): Constraints on the tectonics of the Intrapontide suture zone. *Journal of Asian Earth Sciences*, *171*, 277–288. https://doi.org/10.1016/j.jseaes.2018.11.017

Dickinson, W. R. (1985). Interpreting provenance relations from detrital modes of sandstones. In G. G. Zuffa (Ed.), *Provenance of Arenites* (pp. 333–361). Dordrecht: Reidel.

Dickinson, W. R., & Suczek, C. A. (1979). Plate Tectonics and Sandstone Compositions. *AAPG Bulletin*, *63*(12), 2164–2182.

Dilek, Y., & Altunkaynak, Ş. (2009). Geochemical and temporal evolution of Cenozoic magmatism in western Turkey: mantle response to collision, slab break-off, and lithospheric tearing in an orogenic belt. *Geological Society, London, Special Publications*, *311*(1), 213–233. https://doi.org/10.1144/SP311.8

Dilek, Y., Thy, P., Hacker, B., & Grundvig, S. (1999). Structure and petrology of Tauride ophiolites and mafic dike intrusions (Turkey): Implications for the Neotethyan ocean. *Geological Society of America Bulletin*, 25.

Ding, L., Kapp, P., & Wan, X. (2005). Paleocene–Eocene record of ophiolite obduction and initial India-Asia collision, south central Tibet. *Tectonics*, *24*(3). https://doi.org/10.1029/2004TC001729

Ding, L., Qasim, M., Jadoon, I. A. K., Khan, M. A., Xu, Q., Cai, F., et al. (2016). The India–Asia collision in north Pakistan: Insight from the U–Pb detrital zircon provenance of Cenozoic foreland basin. *Earth and Planetary Science Letters*, *455*, 49–61. https://doi.org/10.1016/j.epsl.2016.09.003

Duru, M., & Aksay, A. (2002). Geological map of the Adapazari quadrangle (Sheet H 24, Scale 1:100,000). Ankara, Turkey: Maden Tetkik ve Arma Genel Müdürlüğü.

Ersoy, E. Y., Palmer, M. R., Genç, Ş. C., Prelević, D., Akal, C., & Uysal, İ. (2017). Chemo-probe into the mantle origin of the NW Anatolia Eocene to Miocene volcanic rocks: Implications for the role of, crustal accretion, subduction, slab roll-back and slab break-off processes in genesis of post-collisional magmatism. *Lithos*, *288–289*, 55–71. https://doi.org/10.1016/j.lithos.2017.07.006

Ersoy, E. Y., Akal, C., Genç, Ş. C., Candan, O., Palmer, M. R., Prelević, D., et al. (2017). U-Pb zircon geochronology of the Paleogene – Neogene volcanism in the NW Anatolia: Its implications for the Late Mesozoic-Cenozoic geodynamic evolution of the Aegean. *Tectonophysics*, *717*, 284–301. https://doi.org/10.1016/j.tecto.2017.08.016

Garzanti, E., Radeff, G., & Malusà, M. G. (2018). Slab breakoff: A critical appraisal of a geological theory as applied in space and time. *Earth-Science Reviews*, *177*, 303–319. https://doi.org/10.1016/j.earscirev.2017.11.012

Gedik, I., & Aksay, A. (2002). Geological map of the Adapazari quadrangle (Sheet H 25, Scale 1:100,000). Ankara, Turkey: Maden Tetkik ve Arma Genel Müdürlüğü.

Gehrels, G. (2012). Detrital Zircon U-Pb Geochronology: Current Methods and New Opportunities. In C. Busby & A. Azor (Eds.), *Tectonics of Sedimentary Basins* (pp. 45–62). Chichester, UK: John Wiley & Sons, Ltd. https://doi.org/10.1002/9781444347166.ch2

Gehrels, G. (2014). Detrital Zircon U-Pb Geochronology Applied to Tectonics. *Annual Review of Earth and Planetary Sciences*, *42*(1), 127–149. https://doi.org/10.1146/annurev-earth-050212-124012

Genç, Ş. C., & Tüysüz, O. (2010). Tectonic setting of the Jurassic bimodal magmatism in the Sakarya Zone (Central and Western Pontides), Northern Turkey: A geochemical and isotopic approach. *Lithos*, *118*(1), 95–111. https://doi.org/10.1016/j.lithos.2010.03.017

Göğüş, O. H., Pysklywec, R. N., & Faccenna, C. (2016). Postcollisional lithospheric evolution of the Southeast Carpathians: Comparison of geodynamical models and observations. *Tectonics*, *35*(5), 1205–1224. https://doi.org/10.1002/2015TC004096

Göncüoğlu, M. C. (2010). *Introduction to the Geology of Turkey: Geodynamic evolution of the pre-Alpine and Alpine terranes*. General Directorate of Mineral Research and Exploration. Retrieved from http://www.academia.edu/download/31280681/MTA_Monogr_Ing_Geology_of_Turkey.pdf

Göncüoğlu, M. C., Turhan, N., Şentürk, K., Özcan, A., Uysal, Ş., & Yaliniz, M. K. (2000). A Geotraverse Across Northwestern Turkey: Tectonic Units of the Central Sakarya Region and their Tectonic Evolution. *Geological Society, London, Special Publications*, *173*(1), 139–161. https://doi.org/10.1144/GSL.SP.2000.173.01.06

Göncüoğlu, M. C., Sayit, K., & Tekin, U. K. (2010). Oceanization of the northern Neotethys: Geochemical evidence from ophiolitic melange basalts within the İzmir–Ankara suture belt, NW Turkey. *Lithos*, *116*(1), 175–187. https://doi.org/10.1016/j.lithos.2010.01.007

Göncüoğlu, M. C., Marroni, M., Pandolfi, L., Ellero, A., Ottria, G., Catanzariti, R., et al. (2014). The Arkot Dağ Mélange in Araç area, central Turkey: Evidence of its origin within the geodynamic evolution of the Intra-Pontide suture zone. *Journal of Asian Earth Sciences*, *85*, 117–139. https://doi.org/10.1016/j.jseaes.2014.01.013

Graham, D. J., & Midgley, N. G. (2000). Graphical representation of particle shape using triangular diagrams: an Excel spreadsheet method. *Earth Surface Processes and Landforms*, *25*(13), 1473–1477. https://doi.org/10.1002/1096-9837(200012)25:13<1473::AID-ESP158>3.0.CO;2-C

Harris, N. B. W., Kelley, S., & Okay, A. I. (1994). Post-collisional magmatism and tectonics in northwest Anatolia. *Contributions to Mineralogy and Petrology*, *117*(3), 241–252.

van Hinsbergen, D. J. J., Kaymakci, N., Spakman, W., & Torsvik, T. H. (2010). Reconciling the geological history of western Turkey with plate circuits and mantle tomography. *Earth and Planetary Science Letters*, *297*(3–4), 674–686. https://doi.org/10.1016/j.epsl.2010.07.024

van Hinsbergen, D. J. J., Kapp, P., Dupont-Nivet, G., Lippert, P. C., DeCelles, P. G., & Torsvik, T. H. (2011). Restoration of Cenozoic deformation in Asia and the size of Greater India. *Tectonics*, *30*(5). https://doi.org/10.1029/2011TC002908

van Hinsbergen, D. J. J., Lippert, P. C., Dupont-Nivet, G., McQuarrie, N., Doubrovine, P. V., Spakman, W., & Torsvik, T. H. (2012). Greater India Basin hypothesis and a two-stage Cenozoic collision between India and Asia. *Proceedings of the National Academy of Sciences*, *109*(20), 7659–7664. https://doi.org/10.1073/pnas.1117262109

van Hinsbergen, D. J. J., Torsvik, T. H., Schmid, S. M., Maţenco, L. C., Maffione, M., Vissers, R. L. M., et al. (2020). Orogenic architecture of the Mediterranean region and kinematic reconstruction of its tectonic evolution since the Triassic. *Gondwana Research*, *81*, 79–229. https://doi.org/10.1016/j.gr.2019.07.009

Hu, X., Garzanti, E., Wang, J., Huang, W., An, W., & Webb, A. (2016). The timing of India-Asia collision onset – Facts, theories, controversies. *Earth-Science Reviews*, *160*, 264–299. https://doi.org/10.1016/j.earscirev.2016.07.014

Jagoutz, O., Royden, L., Holt, A. F., & Becker, T. W. (2015). Anomalously fast convergence of India and Eurasia caused by double subduction. *Nature Geoscience*, *8*(6), 475–478. https://doi.org/10.1038/ngeo2418

Jagoutz, O., Macdonald, F. A., & Royden, L. (2016). Low-latitude arc–continent collision as a driver for global cooling. *Proceedings of the National Academy of Sciences*, *113*(18), 4935–4940. https://doi.org/10.1073/pnas.1523667113

Jones, C. H., Sonder, L. J., & Unruh, J. R. (1998). Lithospheric gravitational potential energy and past orogenesis: Implications for conditions of initial Basin and Range and Laramide deformation, 4.

Jones, C. H., Farmer, G. L., Sageman, B., & Zhong, S. (2011). Hydrodynamic mechanism for the Laramide orogeny. *Geosphere, 7*(1), 183–201. https://doi.org/10.1130/GES00575.1

Jones, M. F., Coster, P. M. C., Licht, A., Métais, G., Ocakoğlu, F., Taylor, M. H., & Beard, K. C. (2018). A stem bat (Chiroptera: Palaeochiropterygidae) from the late middle Eocene of northern Anatolia: implications for the dispersal and palaeobiology of early bats. *Palaeobiodiversity and Palaeoenvironments*. https://doi.org/10.1007/s12549-018-0338-z

Kapp, P., & DeCelles, P. G. (2019). Mesozoic–Cenozoic geological evolution of the Himalayan-Tibetan orogen and working tectonic hypotheses. *American Journal of Science, 319*(3), 159–254. https://doi.org/10.2475/03.2019.01

Kappelman, J., Maas, M. C., Sen, S., Alpagut, B., Fortelius, M., & Lunkka, J.-P. (1996). A new early Tertiary mammalian fauna from Turkey and its paleobiogeographic significance. *Journal of Vertebrate Paleontology, 16*(3), 592–595. https://doi.org/10.1080/02724634.1996.10011345

Kasapoğlu, B., Ersoy, Y. E., Uysal, İ., Palmer, M. R., Zack, T., Koralay, E. O., & Karlsson, A. (2016). The petrology of Paleogene volcanism in the Central Sakarya, Nallıhan Region: Implications for the initiation and evolution of post-collisional, slab break-off-related magmatic activity. *Lithos, 246–247*, 81–98. https://doi.org/10.1016/j.lithos.2015.12.024

Kaymakci, N., Özçelik, Y., White, S. H., & Van Dijk, P. M. (2009). Tectono-stratigraphy of the Çankırı Basin: Late Cretaceous to early Miocene evolution of the Neotethyan Suture Zone in Turkey. *Geological Society, London, Special Publications, 311*(1), 67–106. https://doi.org/10.1144/SP311.3

Keskin, M., & Tüysüz, O. (2018). Stratigraphy, petrogenesis and geodynamic setting of Late Cretaceous volcanism on the SW margin of the Black Sea, Turkey. *Geological Society, London, Special Publications, 464*(1), 95–130. https://doi.org/10.1144/SP464.5

Koshnaw, R. I., Stockli, D. F., & Schlunegger, F. (2019). Timing of the Arabia-Eurasia continental collision—Evidence from detrital zircon U-Pb geochronology of the Red Bed Series strata of the northwest Zagros hinterland, Kurdistan region of Iraq. *Geology, 47*(1), 47–50. https://doi.org/10.1130/G45499.1

Leary, R., Orme, D. A., Laskowski, A. K., DeCelles, P. G., Kapp, P., Carrapa, B., & Dettinger, M. (2016). Along-strike diachroneity in deposition of the Kailas Formation in central southern Tibet: Implications for Indian slab dynamics. *Geosphere, 12*(4), 1198–1223. https://doi.org/10.1130/GES01325.1

Lefebvre, C., Meijers, M. J. M., Kaymakci, N., Peynircioğlu, A., Langereis, C. G., & van Hinsbergen, D. J. J. (2013). Reconstructing the geometry of central Anatolia during the

late Cretaceous: Large-scale Cenozoic rotations and deformation between the Pontides and Taurides. *Earth and Planetary Science Letters*, *366*, 83–98. https://doi.org/10.1016/j.epsl.2013.01.003

Licht, A., Coster, P., Ocakoğlu, F., Campbell, C., Métais, G., Mulch, A., et al. (2017). Tectono-stratigraphy of the Orhaniye Basin, Turkey: Implications for collision chronology and Paleogene biogeography of central Anatolia. *Journal of Asian Earth Sciences*, *143*, 45–58. https://doi.org/10.1016/j.jseaes.2017.03.033

Licht, A., Dupont-Nivet, G., Win, Z., Swe, H. H., Kaythi, M., Roperch, P., et al. (2018). Paleogene evolution of the Burmese forearc basin and implications for the history of India-Asia convergence. *GSA Bulletin*, *5–6*, 730–748. https://doi.org/10.1130/B35002.1

Lygina, E. A., Fokin, P. A., Kopaevich, L. F., Nikishin, A. M., & Yakovishina, E. V. (2016). Nummulitic facies of the Crimean-Caucasian Region. *Turkish Journal of Earth Sciences*, *25*, 163–178. https://doi.org/10.3906/yer-1404-20

Maas, M. C., Thewissen, J. G. M., Sen, S., Kazanci, N., & Kappelman, J. (2001). Enigmatic new ungulates from the Early Middle Eocene of central Anatolia, Turkey. *Journal of Vertebrate Paleontology*, *21*(3), 578–590. https://doi.org/10.1671/0272-4634(2001)021[0578:ENUFTE]2.0.CO;2

Martin, C. R., Jagoutz, O., Upadhyay, R., Royden, L. H., Eddy, M. P., Bailey, E., et al. (2020). Paleocene latitude of the Kohistan–Ladakh arc indicates multistage India–Eurasia collision. *Proceedings of the National Academy of Sciences*. https://doi.org/10.1073/pnas.2009039117

McLean, N. M., Bowring, J. F., & Gehrels, G. (2016). Algorithms and software for U-Pb geochronology by LA-ICPMS. *Geochemistry, Geophysics, Geosystems*, *17*(7), 2480–2496. https://doi.org/10.1002/2015GC006097

McQuarrie, N., & van Hinsbergen, D. J. J. (2013). Retrodeforming the Arabia-Eurasia collision zone: Age of collision versus magnitude of continental subduction. *Geology*, *41*(3), 315–318. https://doi.org/10.1130/G33591.1

McQuarrie, N., Stock, J. M., Verdel, C., & Wernicke, B. P. (2003). Cenozoic evolution of Neotethys and implications for the causes of plate motions. *Geophysical Research Letters*, *30*(20). https://doi.org/10.1029/2003GL017992

Meijers, M. J. M., Kaymakci, N., Hinsbergen, D. J. J. van, Langereis, C. G., Stephenson, R. A., & Hippolyte, J.-C. (2010). Late Cretaceous to Paleocene oroclinal bending in the central Pontides (Turkey). *Tectonics*, *29*(4). https://doi.org/10.1029/2009TC002620

Métais, G., Beard, K., Erdal, O., & Erturaç, K. (2017). Tarsal morphology of the pleuraspidotheriid mammal Hilalia from the middle Eocene of Turkey. *Acta Palaeontologica Polonica*, *62*. https://doi.org/10.4202/app.00314.2016

Métais, G., Coster, P. M., Kappelman, J. R., Licht, A., Ocakoglu, F., Taylor, M. H., & Beard, K. C. (2018). Eocene metatherians from Anatolia illuminate the assembly of an island fauna during Deep Time. *PLoS ONE*, *13*(11), e0206181.

MTA. (2002). Geological map of Turkey, scale 1:500,000. *Mineral Research and Exploration Institute of Turkey*.

Mueller, M. A., Licht, A., Campbell, C., Ocakoğlu, F., Taylor, M. H., Burch, L., et al. (2019). Collision Chronology Along the İzmir-Ankara-Erzincan Suture Zone: Insights From the Sarıcakaya Basin, Western Anatolia. *Tectonics*, *38*(10), 3652–3674. https://doi.org/10.1029/2019TC005683

Najman, Y., Appel, E., Boudagher-Fadel, M., Bown, P., Carter, A., Garzanti, E., et al. (2010). Timing of India-Asia collision: Geological, biostratigraphic, and palaeomagnetic constraints. *Journal of Geophysical Research: Solid Earth*, *115*(B12). https://doi.org/10.1029/2010JB007673

Niu, Y. (2017). Slab breakoff: a causal mechanism or pure convenience? *Science Bulletin*, *62*(7), 456–461. https://doi.org/10.1016/j.scib.2017.03.015

Ocakoğlu, F., Yılmaz, İ. Ö., Demircan, H., Altıner, S. Ö., Hakyemez, A., İslamoğlu, Y., et al. (2007). Orta Sakarya Bölgesi Geç Kretase-Paleojen Çökellerinin Sekans Stratigrafisi. *The Scientific and Technological Research Council of Turkey (TUBİTAK, Project no: 104Y153), Final Report*, 476.

Ocakoğlu, F., Açıkalın, S., Yılmaz, I. ö., Şafak, ü., & Gökçeoğlu, C. (2012). Evidence of orbital forcing in lake-level fluctuations in the Middle Eocene oil shale-bearing lacustrine successions in the Mudurnu-Göynük Basin, NW Anatolia (Turkey). *Journal of Asian Earth Sciences*, *56*, 54–71. https://doi.org/10.1016/j.jseaes.2012.04.021

Ocakoğlu, F., Hakyemez, A., Açıkalın, S., Özkan Altıner, S., Büyükmeriç, Y., Licht, A., et al. (2018). Chronology of subduction and collision along the İzmir-Ankara suture in Western Anatolia: records from the Central Sakarya Basin. *International Geology Review*, 1–26. https://doi.org/10.1080/00206814.2018.1507009

Okay, A. (2011). Tavsanli Zone: The Northern Subducted Margin Of The Anatolide-Tauride Block. *Mineral Res. Expl. Bull.*, *142*, 191–221.

Okay, A., & Satir, M. (2006). Geochronology of Eocene plutonism and metamorphism in northwest. *Geodinamica Acta*, *19*(5), 251–266. https://doi.org/10.3166/ga.19.251-266

Okay, A., Satir, M., maluski, H., SIYAKO, M., Monie, P., Metzger, R., & Akyüz, S. (1996). Paleo- and Neo-Tethyan events in northwestern Turkey: Geologic and geochronologic constraints. *Cambridge University Press*, 420–441.

Okay, A., Harris, N. B. W., & Kelley, S. P. (1998). Exhumation of blueschists along a Tethyan suture in northwest Turkey. *Tectonophysics*, *285*(3–4), 275–299. https://doi.org/10.1016/S0040-1951(97)00275-8

Okay, A. I., & Göncüoglu, M. C. (2004). The Karakaya Complex: A Review of Data and Concepts. *Turkish Journal of Earth Sciences*, *13*(2), 77–95.

Okay, A. I., & Nikishin, A. M. (2015). Tectonic evolution of the southern margin of Laurasia in the Black Sea region. *International Geology Review*, *57*(5–8), 1051–1076. https://doi.org/10.1080/00206814.2015.1010609

Okay, A. I., & Whitney, D. L. (2010). Blueschists, Eclogites, Ophiolites and Suture Zones in Northwest Turkey: A Review and a Field Excursion Guide. *Ofioliti*, *35*(2), 131–172.

Okay, A. I., Şengör, A. M. C., & Görür, N. (1994). Kinematic history of the opening of the Black Sea and its effect on the surrounding regions. *Geology*, *22*(3), 267–270. https://doi.org/10.1130/0091-7613(1994)022<0267:KHOTOO>2.3.CO;2

Okay, A. I., Tansel, I., & TüYsüZ, O. (2001). Obduction, subduction and collision as reflected in the Upper Cretaceous–Lower Eocene sedimentary record of western Turkey. *Geological Magazine*, *138*(02). https://doi.org/10.1017/S0016756801005088

Okay, A. I., Zattin, M., & Cavazza, W. (2010). Apatite fission-track data for the Miocene Arabia-Eurasia collision. *Geology*, *38*(1), 35–38. https://doi.org/10.1130/G30234.1

Okay, A. I., Sunal, G., Sherlock, S., Altiner, D., Tüysüz, O., Kylander-Clark, A. R. C., & Aygül, M. (2013). Early Cretaceous sedimentation and orogeny on the active margin of Eurasia: Southern Central Pontides, Turkey. *Tectonics*, *32*(5), 1247–1271. https://doi.org/10.1002/tect.20077

Özcan, E., Özcan, Z., Okay, A. I., Akbayram, K., & Hakyemez, A. (2019). The Ypresian to Lutetian marine record in NW Turkey: a revised biostratigraphy and chronostratigraphy and implications for Eocene paleogeography. *Turkish Journal of Earth Sciences*, *28*, 27.

Özcan, Z., Okay, A. I., Özcan, E., Hakyemez, A., & Özkan-Altiner, S. (2012). Late Cretaceous–Eocene Geological Evolution of the Pontides Based on New Stratigraphic and Palaeontologic Data Between the Black Sea Coast and Bursa (NW Turkey). *Turkish Journal of Earth Sciences*, *21*, 933–960. https://doi.org/10.3906/yer-1102-8

Özgen-Erdem, N., Akyazı, M., & Karabaşoğlu, A. (2007). Biostratigraphic interpretation and systematics of Alveolina assemblages from the Ilerdian–Cuisian limestones of Southern Eskişehir, Central Turkey. *Journal of Asian Earth Sciences*, *29*(5), 911–927. https://doi.org/10.1016/j.jseaes.2006.05.010

Parker, S. D., & Pearson, D. M. (2021). Pre-Thrusting Stratigraphic Control on the Transition From a Thin-Skinned to Thick-Skinned Structural Style: An Example From the Double-

Decker Idaho-Montana Fold-Thrust Belt. *Tectonics*, *40*(5), e2020TC006429. https://doi.org/10.1029/2020TC006429

Paterson, S. R., & Ducea, M. N. (2015). Arc Magmatic Tempos: Gathering the Evidence. *Elements*, *11*(2), 91–98. https://doi.org/10.2113/gselements.11.2.91

Paton, C., Hellstrom, J., Paul, B., Woodhead, J., & Hergt, J. (2011). Iolite: Freeware for the visualisation and processing of mass spectrometric data. *Journal of Analytical Atomic Spectrometry*, *26*(12), 2508. https://doi.org/10.1039/c1ja10172b

Plunder, A., Agard, P., Chopin, C., & Okay, A. (2013). Tectono-metamorphic evolution of the Tavşanli zone, Western Anatolia: implications for mechanical coupling during subduction/obduction processes (Vol. 15, pp. EGU2013-8404). Presented at the EGU General Assembly Conference Abstracts. Retrieved from http://adsabs.harvard.edu/abs/2013EGUGA..15.8404P

Plunder, A., Agard, P., Chopin, C., Pourteau, A., & Okay, A. I. (2015). Accretion, underplating and exhumation along a subduction interface: From subduction initiation to continental subduction (Tavşanlı zone, W. Turkey). *Lithos*, *226*, 233–254. https://doi.org/10.1016/j.lithos.2015.01.007

Pourteau, A., Sudo, M., Candan, O., Lanari, P., Vidal, O., & Oberhänsli, R. (2013). Neotethys closure history of Anatolia: insights from ^{40}Ar-^{39}Ar geochronology and *P-T* estimation in high-pressure metasedimentary rocks. *Journal of Metamorphic Geology*, *31*(6), 585–606. https://doi.org/10.1111/jmg.12034

Pourteau, A., Oberhänsli, R., Candan, O., Barrier, E., & Vrielynck, B. (2016). Neotethyan closure history of western Anatolia: a geodynamic discussion. *International Journal of Earth Sciences*, *105*(1), 203–224. https://doi.org/10.1007/s00531-015-1226-7

Pourteau, A., Scherer, E. E., Schorn, S., Bast, R., Schmidt, A., & Ebert, L. (2019). Thermal evolution of an ancient subduction interface revealed by Lu–Hf garnet geochronology, Halilbağı Complex (Anatolia). *Geoscience Frontiers*, *10*(1), 127–148. https://doi.org/10.1016/j.gsf.2018.03.004

Racey, A. (2001). A review of Eocene nummulite accumulations: Structure, formation and reservoir potential. *Journal of Petroleum Geology*, *24*(1), 79–100. https://doi.org/10.1111/j.1747-5457.2001.tb00662.x

Robertson, A. H. F., & Ustaömer, T. (2004). Tectonic evolution of the Intra-Pontide suture zone in the Armutlu Peninsula, NW Turkey. *Tectonophysics*, *381*(1–4), 175–209. https://doi.org/10.1016/j.tecto.2002.06.002

Robertson, A. H. F., Parlak, O., & Ustaömer, T. (2009). Melange genesis and ophiolite emplacement related to subduction of the northern margin of the Tauride–Anatolide continent, central and western Turkey. *Geological Society, London, Special Publications*, *311*(1), 9–66. https://doi.org/10.1144/SP311.2

Şahin, M., Yaltırak, C., & Karacık, Z. (2019). A case study of compression to escape tectonic transition: Tectonic evolution of the Nallıhan Wedge and comparison with the Tercan Wedge (Eastern Mediterranean, Turkey). *Journal of Asian Earth Sciences*, *174*, 311–331. https://doi.org/10.1016/j.jseaes.2018.12.016

Sarıfakıoğlu, E., Özen, H., & Winchester, J. A. (2009). Whole Rock and Mineral Chemistry of Ultramafic-mafic Cumulates from the Orhaneli (Bursa) Ophiolite, NW Anatolia. *Turkish Journal of Earth Sciences*, *18*, 55–83. https://doi.org/10.3906/yer-0806-8

Sarıfakıoğlu, E., Dilek, Y., & Sevin, M. (2017). New synthesis of the Izmir-Ankara-Erzincan suture zone and the Ankara mélange in northern Anatolia based on new geochemical and geochronological constraints. In R. Sorkhabi (Ed.), *Tectonic Evolution, Collision, and Seismicity of Southwest Asia: In Honor of Manuel Berberian's Forty-Five Years of Research Contributions* (Vol. 525, pp. 1–63). Retrieved from https://doi.org/10.1130/2017.2525(19)

Schleiffarth, W. K., Darin, M. H., Reid, M. R., & Umhoefer, P. J. (2018). Dynamics of episodic Late Cretaceous–Cenozoic magmatism across Central to Eastern Anatolia: New insights from an extensive geochronology compilation. *Geosphere*, *14*(5), 1990–2008. https://doi.org/10.1130/GES01647.1

Seaton, N. C. A., Whitney, D. L., Teyssier, C., Toraman, E., & Heizler, M. T. (2009). Recrystallization of high-pressure marble (Sivrihisar, Turkey). *Tectonophysics*, *479*(3), 241–253. https://doi.org/10.1016/j.tecto.2009.08.015

Sen, S. (2013). Dispersal of African mammals in Eurasia during the Cenozoic: Ways and whys. *Geobios*, *46*(1–2), 159–172. https://doi.org/10.1016/j.geobios.2012.10.012

Şengör, A. M. C., & Yilmaz, Y. (1981). Tethyan evolution of turkey: a plate tectonic approach. *Tectonophysics*, *75*, 181–241.

Sharman, G. R., Sharman, J. P., & Sylvester, Z. (2018). detritalPy: A Python-based toolset for visualizing and analysing detrital geo-thermochronologic data. *The Depositional Record*, *4*(2), 202–215. https://doi.org/10.1002/dep2.45

Shekut, S., & Licht, A. (2020). Late Middle Miocene Emergence of the Olympic Peninsula Shown by Sedimentary Provenance. *Lithosphere*, *2020*(1), 1–20. https://doi.org/10.2113/2020/7040598

Sherlock, S., Kelley, S., Inger, S., Harris, N., & Okay, A. (1999). 40Ar-39Ar and Rb-Sr geochronology of high-pressure metamorphism and exhumation history of the Tavsanli Zone, NW Turkey. *Contributions to Mineralogy and Petrology*, *137*(1–2), 46–58. https://doi.org/10.1007/PL00013777

Sinclair, H. D. (1997). Flysch to molasse transition in peripheral foreland basins: The role of the passive margin versus slab breakoff. *Geology*, *25*(12), 1123–1126.

Soret, M., Larson, K. P., Cottle, J., & Ali, A. (2021). How Himalayan collision stems from subduction. *Geology*. https://doi.org/10.1130/G48803.1

Speciale, P. A., Catlos, E. J., Yıldız, G. O., Shin, T. A., & Black, K. N. (2012). Zircon ages from the Beypazarı granitoid pluton (north central Turkey): tectonic implications. *Geodinamica Acta*, *25*(3–4), 162–182. https://doi.org/10.1080/09853111.2013.858955

Timur, E., & Aksay, A. (2002). Geological map of the Adapazari quadrangle (Sheet H 26, Scale 1:100,000). Ankara, Turkey: Maden Tetkik ve Arma Genel Müdürlüğü.

Turhan, N. (2002). Geologic map of Turkey (Ankara, Scale 1:500,000). Ankara, Turkey: Maden Tetkik ve Arma Genel Müdürlüğü.

Tye, A. R., Niemi, N. A., Safarov, R. T., Kadirov, F. A., & Babayev, G. R. (2020). Sedimentary response to a collision orogeny recorded in detrital zircon provenance of Greater Caucasus foreland basin sediments. *Basin Research*, *n/a*(n/a). https://doi.org/10.1111/bre.12499

Ustaömer, P., Ustaömer, T., & Robertson, Alastair. H. F. (2012). Ion Probe U-Pb Dating of the Central Sakarya Basement: A peri-Gondwana Terrane Intruded by Late Lower Carboniferous Subduction/Collision-related Granitic Rocks. *Turkish Journal of Earth Sciences*, *21*(6), 905–932. https://doi.org/10.3906/yer-1103-1

Ustaömer, P. A., Ustaömer, T., Collins, A. S., & Reischpeitsch, J. (2009). Lutetian arc-type magmatism along the southern Eurasian margin: New U-Pb LA-ICPMS and whole-rock geochemical data from Marmara Island, NW Turkey. *Mineralogy and Petrology*, *96*(3), 177–196. https://doi.org/10.1007/s00710-009-0051-8

Ustaömer, T., Ustaömer, P., Robertson, A. H. F., & Gerdes, A. (2016). Implications of U–Pb and Lu–Hf isotopic analysis of detrital zircons for the depositional age, provenance and tectonic setting of the Permian–Triassic Palaeotethyan Karakaya Complex, NW Turkey. *International Journal of Earth Sciences*, *105*(1), 7–38. https://doi.org/10.1007/s00531-015-1225-8

Whitney, D. L., Teyssier, C., Toraman, E., Seaton, N. C. A., & Fayon, A. K. (2011). Metamorphic and tectonic evolution of a structurally continuous blueschist-to-Barrovian terrane, Sivrihisar Massif, Turkey. *Journal of Metamorphic Geology*, *29*(2), 193–212. https://doi.org/10.1111/j.1525-1314.2010.00915.x

Whitney, Donna L., & Davis, P. B. (2006). Why is lawsonite eclogite so rare? Metamorphism and preservation of lawsonite eclogite, Sivrihisar, Turkey. *Geology*, *34*(6), 473–476. https://doi.org/10.1130/G22259.1

Yaliniz, M. K., Göncüoğlu, M. C., & Ozkan-Altiner, S. (2000). Formation and emplacement ages of the SSZ-type Neotethyan ophiolites in Central Anatolia, Turkey: palaeotectonic implications. *Geological Journal*, *35*(2), 53–68. https://doi.org/10.1002/1099-1034(200004/06)35:2<53::AID-GJ837>3.0.CO;2-6

Yildiz, A., Kibici, Y., Bağci, M., Dumlupunar, İ., Kocabaş, C., & Aritan, A. E. (2015). Petrogenesis of the post-collisional Eocene volcanic rocks from the Central Sakarya Zone (Northwestern Anatolia, Turkey): Implications for source characteristics, magma evolution, and tectonic setting. *Arabian Journal of Geosciences*, *8*(12), 11239–11260. https://doi.org/10.1007/s12517-015-1991-4

Yilmaz, I. O., Altiner, D., Tekin, U. K., Tuysuz, O., Ocakoglu, F., & Acikalin, S. (2010). Cenomanian – Turonian Oceanic Anoxic Event (OAE2) in the Sakarya Zone, northwestern Turkey: Sedimentological, cyclostratigraphic, and geochemical records. *Cretaceous Research*, *31*(2), 207–226. https://doi.org/10.1016/j.cretres.2009.10.005